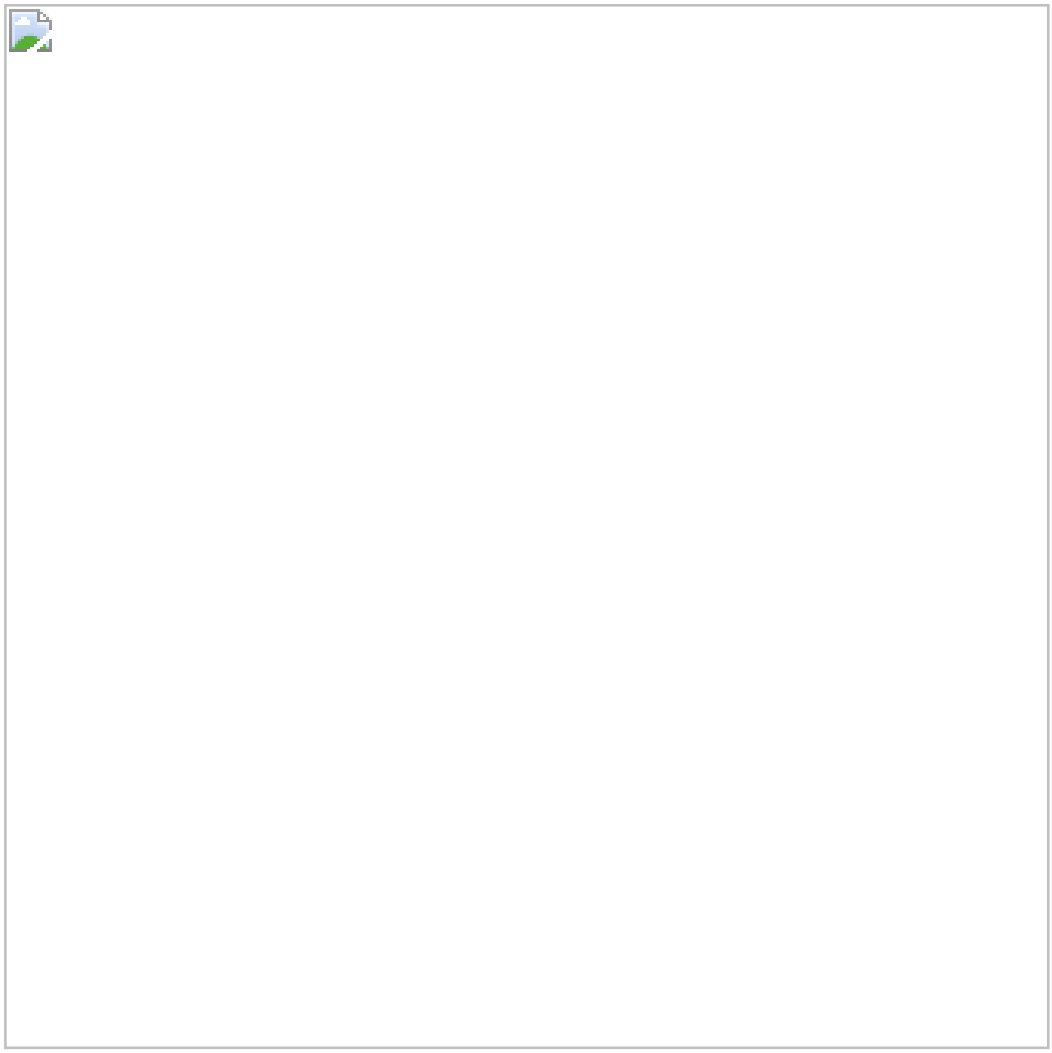

Biodiversity Evolution Through the Permian—Triassic Boundary Event: Ostracods from the Bükk Mountains, Hungary

Authors: Forel, Marie-Béatrice, Crasquin, Sylvie, Hips, Kinga, Kershaw, Steve, Collin, Pierre-Yves, et al.

Source: Acta Palaeontologica Polonica, 58(1) : 195-219

Published By: Institute of Paleobiology, Polish Academy of Sciences

URL: https://doi.org/10.4202/app.2011.0126

Biodiversity evolution through the Permian–Triassic boundary event: Ostracods from the Bükk Mountains, Hungary

MARIE-BÉATRICE FOREL, SYLVIE CRASQUIN, KINGA HIPS, STEVE KERSHAW, PIERRE-YVES COLLIN, and JÁNOS HAAS

Forel, M.-B., Crasquin, S., Hips, K., Kershaw, S., Collin, P.-Y., and Haas, J. 2013. Biodiversity evolution through the Permian–Triassic boundary event: Ostracods from the Bükk Mountains, Hungary. *Acta Palaeontologica Polonica* 58 (1): 195–219.

One of the most complete Permian–Triassic boundary sections located in the Bükk Mountains (Hungary) was sampled for ostracod study. Seventy-six species are recognized, belonging to twenty genera. Fifteen new species are described and figured: *Acratia*? *jeanvannieri* Forel sp. nov., *Acratia nagyvisnyoensis* Forel sp. nov., *Bairdia anisongae* Forel sp. nov., *Bairdia davehornei* Forel sp. nov., *Callicythere*? *balvanyseptentrioensis* Forel sp. nov., *Cytherellina*? *magyarorszagensis* Forel sp. nov., *Eumiraculum desmaresae* Forel sp. nov., *Hollinella fengqinglaii* Crasquin sp. nov., *Hungarella gerennavarensis* Crasquin sp. nov., *Langdaia bullabalvanyensis* Crasquin sp. nov., *Liuzhinia venninae* Forel sp. nov., *Liuzhinia bankutensis* Forel sp. nov., *Microcheilinella egerensis* Forel sp. nov., *Reviya praecurukensis* Forel sp. nov., *Shemonaella*? *olempskaella* Forel sp. nov. One species is renamed: *Bairdia baudini* Crasquin nom. nov. Comparison of the Bálvány North section with the Meishan section (Zhejiang Province, South China), Global Boundary Stratotype Section and Point (GSSP) of the Permian–Triassic Boundary (PTB), reveals discrepancies linked to the environmental setting and particularly to bathymetry. The stratigraphical distribution of all the species is given and diversity variations are discussed. The Bálvány North section exhibits the lowest extinction rate of all PTB sections studied for ostracods analysis associated with a high level of endemism.

Key words: Ostracoda, biodiversity, Permian–Triassic boundary, Bükk Mountains, Hungary.

Marie-Béatrice Forel [mbforel@yahoo.fr], State Key Laboratory of Geological Process and Mineral Resources, China University of Geosciences, Wuhan Hubei, People's Republic of China;
Sylvie Crasquin [sylvie.crasquin@upmc.fr], CNRS-UMR 7207 CR2P, UPMC Université Paris 06, T. 46–56, E. 5, case 104, 75252 Paris cedex 05, France;
Kinga Hips [hips@ludens.elte.hu] and János Haas [haas@ludens.elte.hu], Geological, Geophysical and Space Science Research Group, Hungarian Academy of Sciences, Eötvös University, H-1117 Budapest, Pázmánys; 1/c, Hungary;
Steve Kershaw [stephen.kershaw@brunel.ac.uk], Institute for the Environment, Halsbury Building, Brunel University, Uxbridge, Middlesex, UB8 3PH, UK;
Pierre-Yves Collin [pierre-yves.collin@u-bourgogne.fr], Université de Bourgogne, UMR 6282 Biogéosciences, Bâtiment Sciences Gabriel, 6 Bd Gabriel, 21000 Dijon, France.

Received 26 August 2011, accepted 17 September 2012, available online 16 October 2012.

Introduction

The Permian–Triassic Boundary (PTB) was recognized in several sections of the Bükk Mountains (Northern Hungary) in continuous marine successions. The Bálvány North section (48°06'179N, 20°28'491E) is located on the northern slope of Mount Bálvány, 1 km NW of Bánkút (northern Bükk Mountains) (Fig. 1) and is one of the best known localities for the Permian–Triassic transition. This outcrop was studied in great detail by Haas et al. (2004, 2006, 2007) and Hips and Haas (2006, 2009). These authors described the facies development along the section. Numerous ostracods were observed in thin sections. We sampled this section for ostracod analysis in the framework of a large-scale study on the extinction and recovery of this group through the PTB interval. This research was conducted in South China: Meishan GSSP, Zhejiang Province (Crasquin et al. 2010a; Forel and Crasquin 2011b); Guizhou Province (Forel et al. 2009); Sichuan Province (Crasquin-Soleau and Kershaw 2005); Guangxi Province (Crasquin-Soleau et al. 2006); in Tibet (Crasquin et al. 2007; Forel and

http://dx.doi.org/10.4202/app.2011.0126

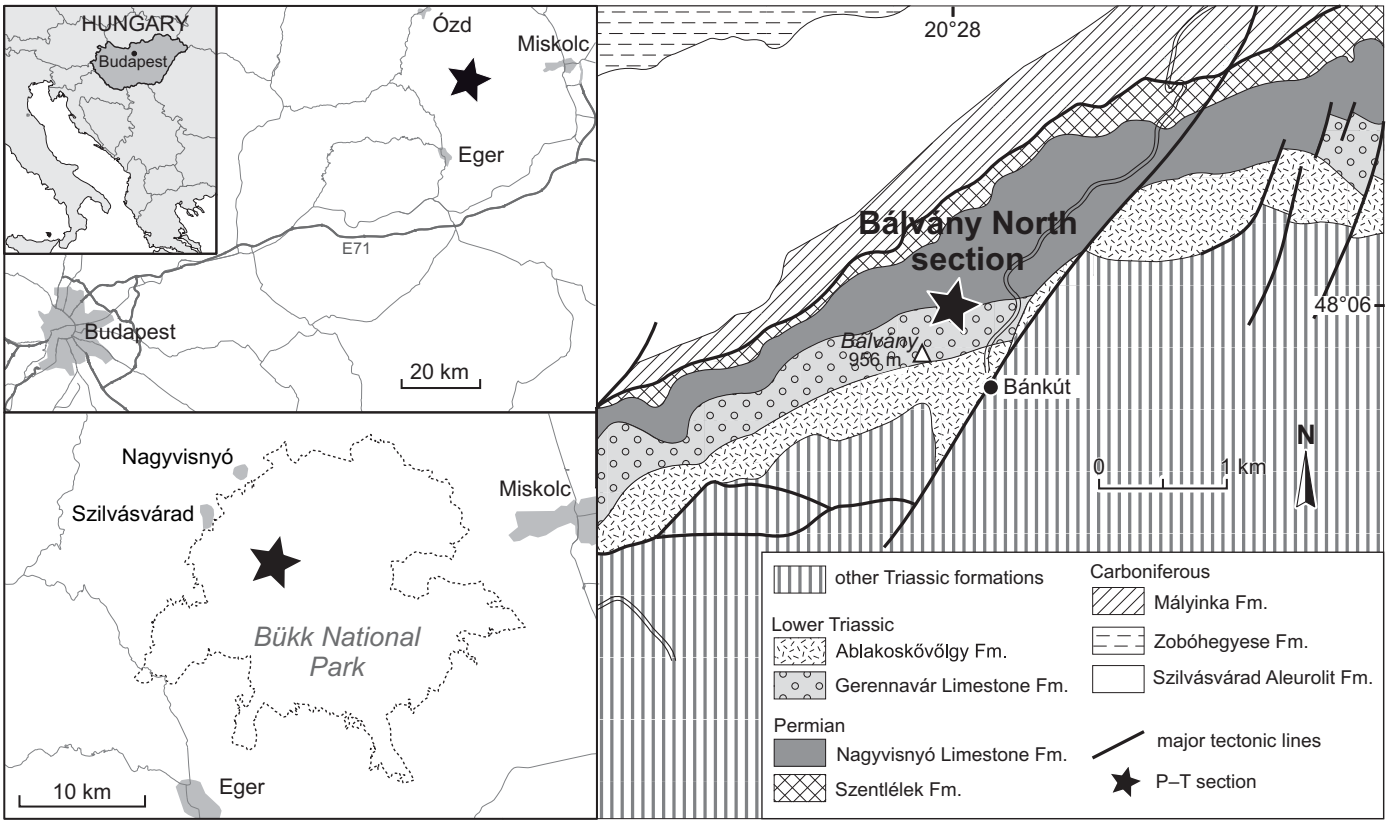

Fig. 1. Location map of the northern part of the Bükk Mountains (after Less et al. 2002) with Bálvány North P–T boundary section. Fm., Formation.

Crasquin 2011a; Forel et al. 2011); in Northern Italy, Bulla section (Crasquin et al. 2008); in SW Taurus, Turkey, Çürük Dağ section (Crasquin-Soleau et al. 2002, 2004a, b). In Hungary, Kozur published a systematic (1985b) and a biostratigraphic evaluation (1985a) of Upper Palaeozoic ostracods from the Bükk Mountains. Here, seventy-six species belonging to twenty genera are recognized and their potential biostratigraphic utility evaluated.

Institutional abbreviations.—UPMC P6M, Université Pierre et Marie Curie, Paris, France.

Other abbreviations.—AB, anterior border; ACA, anterior cardinal angle; ADB, anterodorsal border; AVB, anteroventral border; BSB, Boundary Shale Bed; DB, dorsal border; H, height; Hmax, maximal height; L, length; Lmax, maximal length; LV, left valve; L_1–L_4, lobes; PB, posterior border; PCA, posterior cardinal angle; PDB, posterodorsal border; PVB, posteroventral border; PTB, Permian–Triassic Boundary; RV, right valve; S_2, median sulcus; VB, ventral border.

Geological setting

The Bükk Mountains, located in northern Hungary, to the south of the Western Carpathians, are made up of metamorphosed Palaeozoic–Mesozoic rocks. They are overlain by non-metamorphic Palaeogene–Neogene formations (Less et al. 2002). Permian–Lower Triassic deposits are known only in the northern part of the mountains. In accordance with the purpose of this paper, results of previous studies are only briefly summarized here. For detailed sedimentological description of the section and for discussion of selected topics the reader is referred to the papers by Haas et al. (2004, 2006, 2007), Hips and Haas (2006, 2009), and Sudar et al. (2008).

The studied boundary section is 3.7 m thick (Fig. 2). In the lower part of the section occur dark grey bioclastic limestone beds (wackestone–packstone) with calcareous marlstone interlayers of mid- to outer ramp facies which exhibit a deepening-upward trend (1.35 m; Nagyvisnyó Limestone Formation). In this interval the conodonts *Hindeodus praeparvus* Kozur, 1996 and *Isarcicella* cf. *prisca* Kozur, 1995 were identified (Haas et al. 2007; Sudar et al. 2008) which, along with marine acritarchs, bisaccate and striate pollens (Haas et al. 2004), suggest that these beds are of Permian age. This bedset unit is overlain by thin mudstone beds (0.25 m), recording the first biotic decline, and a circa 1 m thick marly siltstone bed, recording the second biotic decline (Haas et al. 2004). The lower two-thirds of this bed preserve the last

Fig. 2. **A**. Lithological column (after Haas et al. 2007) with the distribution of analysed samples. The ostracod symbols indicate the productive samples. **B**. Stratigraphic occurrence of ostracod species in Bálvány North section, Hungary. Fm., Formation. →

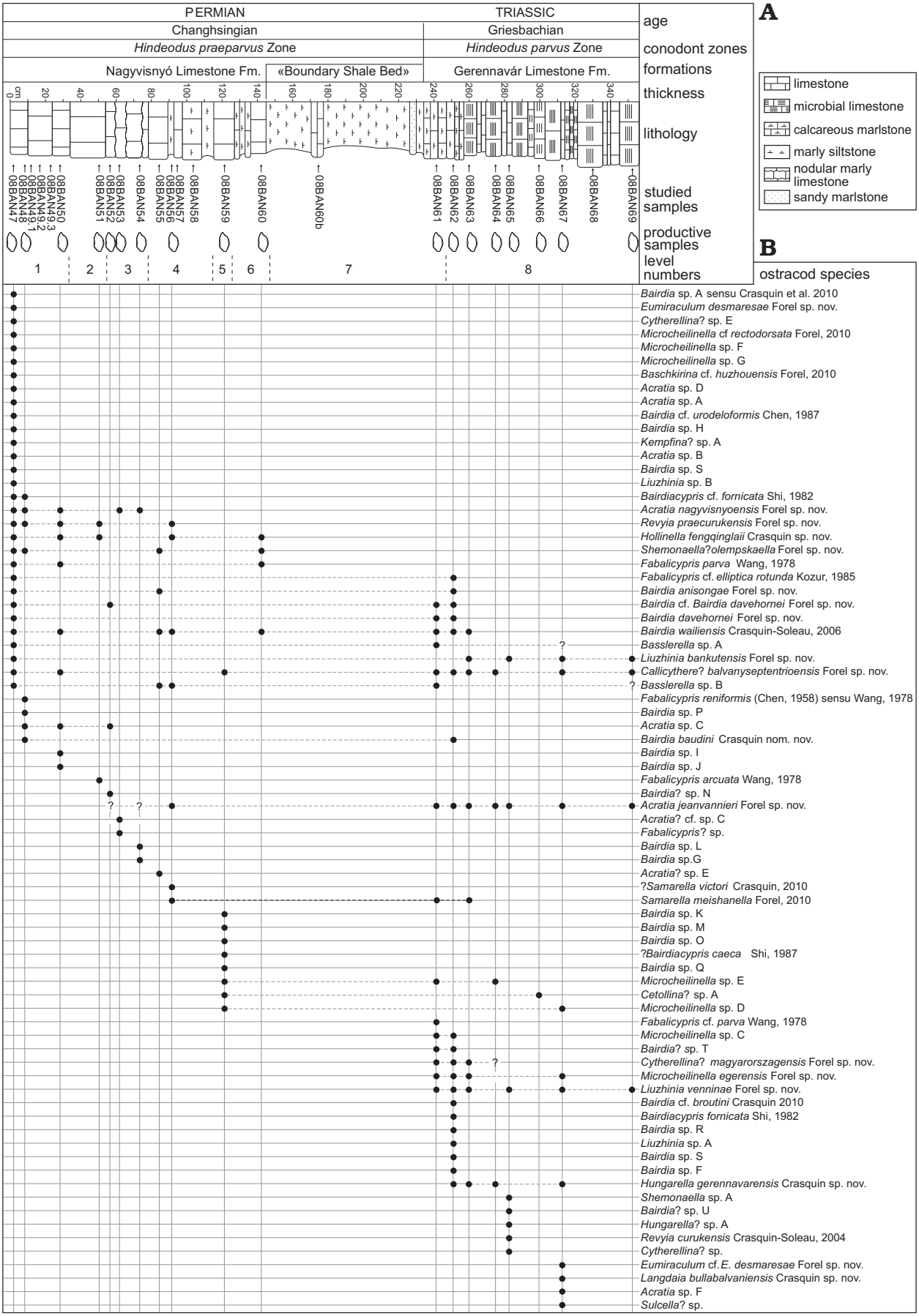

http://dx.doi.org/10.4202/app.2011.0126

Permian bivalve and brachiopod assemblage (Posenato et al. 2005). In addition, carbon isotope values from the bioclastic limestone display a negative shift with a prominent peak in the upper two-third of the BSB (Haas et al. 2006), which is considered as an isotope chemostratigraphic marker (e.g., Erwin et al. 2002). Numerous small cavate spores were encountered from the uppermost part of the BSB suggesting that this interval may be of Triassic age (Haas et al. 2004). The conodont *Hindeodus parvus* (Kozur and Pjatakova, 1976), which is recognised as the marker for the base of the Triassic (Yin et al. 1996, 2001), was found in the lower part of the overlying platy mudstone unit (0.5 m; Gerennavár Limestone Formation). Thus, the first documented occurrence of the conodont *H. parvus* is 0.55 m above the negative peak of the $\delta^{13}C$ curve, and 0.2 m above the Formation boundary (Haas et al. 2007; Sudar et al. 2008). Upsection, planar stromatolites occur (0.6 m in the studied section).

Material and methods

Twenty-five samples have been processed for ostracod analysis (Fig. 2A). The extraction of calcareous ostracod carapaces from calcareous rocks is achieved by hot acetolysis (Lethiers and Crasquin 1988; Crasquin-Soleau et al. 2005). Nineteen samples yielded ostracods (Fig. 2B). Seventy-six species belonging to twenty genera are identified and figured (Figs. 4, 6, 10, 12, 15, 18, 21–23). Fifteen species are new and here described. Nearly all specimens are represented by complete carapaces; this testifies to absence or limitation of post-mortem transportation with low wave energy and/or rapid burial by high sedimentation ratio (Oertli 1971). Some of the described species are presented in open nomenclature because of poor preservation and/or too low number of specimens to differentiate between intraspecific variations and different species. However, we decided to figure all the material recovered because these new data exemplify an unexpected survival phenomenon of microbial origin in a refuge area and are important for the understanding of events following the end-Permian extinction.

Systematic paleontology

(M.-B. Forel and S. Crasquin)

The classification adopted here is from Moore (1961) modified after Bowman and Abele (1982) and Horne et al. (2002).

Phylum Arthropoda Latreille, 1802
Subphylum Crustacea Brünnich, 1772
Class Ostracoda Latreille, 1802
Subclass Podocopa Müller, 1894
Order Palaeocopida Henningsmoen, 1953
Suborder Beyrichicopina Scott, 1961
Superfamily Kirkbyoidea Ulrich and Bassler, 1906
Family Kirkbyidae Ulrich and Bassler, 1906
Genus *Reviya* Sohn, 1961

Type species: *Amphissites*? *obesus* Croneis and Gale, 1939; Upper Mississippian (Carboniferous), Illinois (USA).

Reviya praecurukensis Forel sp. nov.

Fig. 4A–H.

?2010 *Indivisia* cf. *pelikani* Kozur, 1985; Crasquin et al. 2010b: pl. 1: 8.

Etymology: In reference to *Reviya curukensis* Crasquin-Soleau, 2004, which is close in shape and occurs later, in the Lower Triassic.

Type material: Holotype: one complete carapace, Fig. 4A, UPMC P6M2742, sample 08BAN47. Paratype: one complete carapace, Fig. 4B, UPMC P6M2743, sample 08BAN47.

Type locality: Bálvány North section, Bükk Mountains, Hungary.

Type horizon: Level 1, Nagyvisnyó Limestone Formation, Changhsingian, Upper Permian.

Material.—42 complete and 6 broken carapaces, samples 08BAN47, 48, 50, 51, 56 (see Fig. 2B), levels 1, 2, 4, Nagyvisnyó Limestone Formation, Bálvány North section, Hungary, Changhsingian, Upper Permian.

Diagnosis.—A species of *Reviya* with a subquadrangular carapace, a straight to gently convex VB, a small shoulder in the posterodorsal part and an elongated pit near mid-H.

Dimensions (of adults).—L 425–800 μm, H 220–440 μm (see Fig. 3).

Description.—Carapace subrectangular; DB straight and long; ACA and PCA clear and more or less equivalent; AB with large radius of curvature and maximum of curvature located at mid-H; VB straight and long; PB with large radius of curvature, in all the cases a little smaller than AB, with maximum of curvature located above mid-H; presence of small shoulders in postero-dorsal part of the carapace; kirkbyan pit elongated and located at mid-H and mid-L; presence of a subventral ridge parallel to free margin; surface reticulated, on best preserved specimens nodes could be observed along free margins and DB; RV overlaps LV along free margins. Sexual dimorphism expressed in the heteromorphs by enlargement of posterior part of the carapace. Internal features unknown.

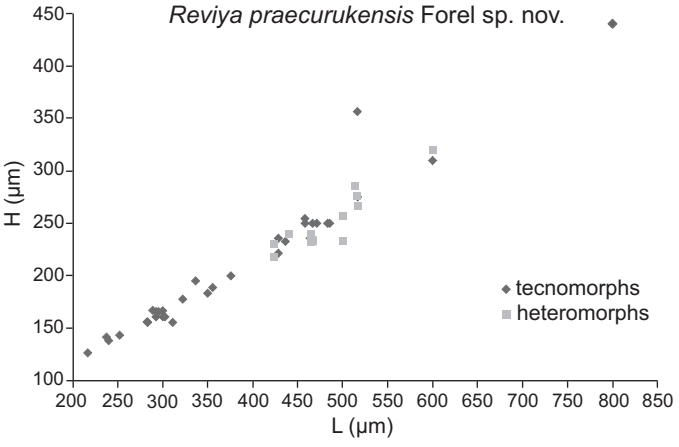

Fig. 3. Height/length diagram of *Reviya praecurukensis* Forel sp. nov.

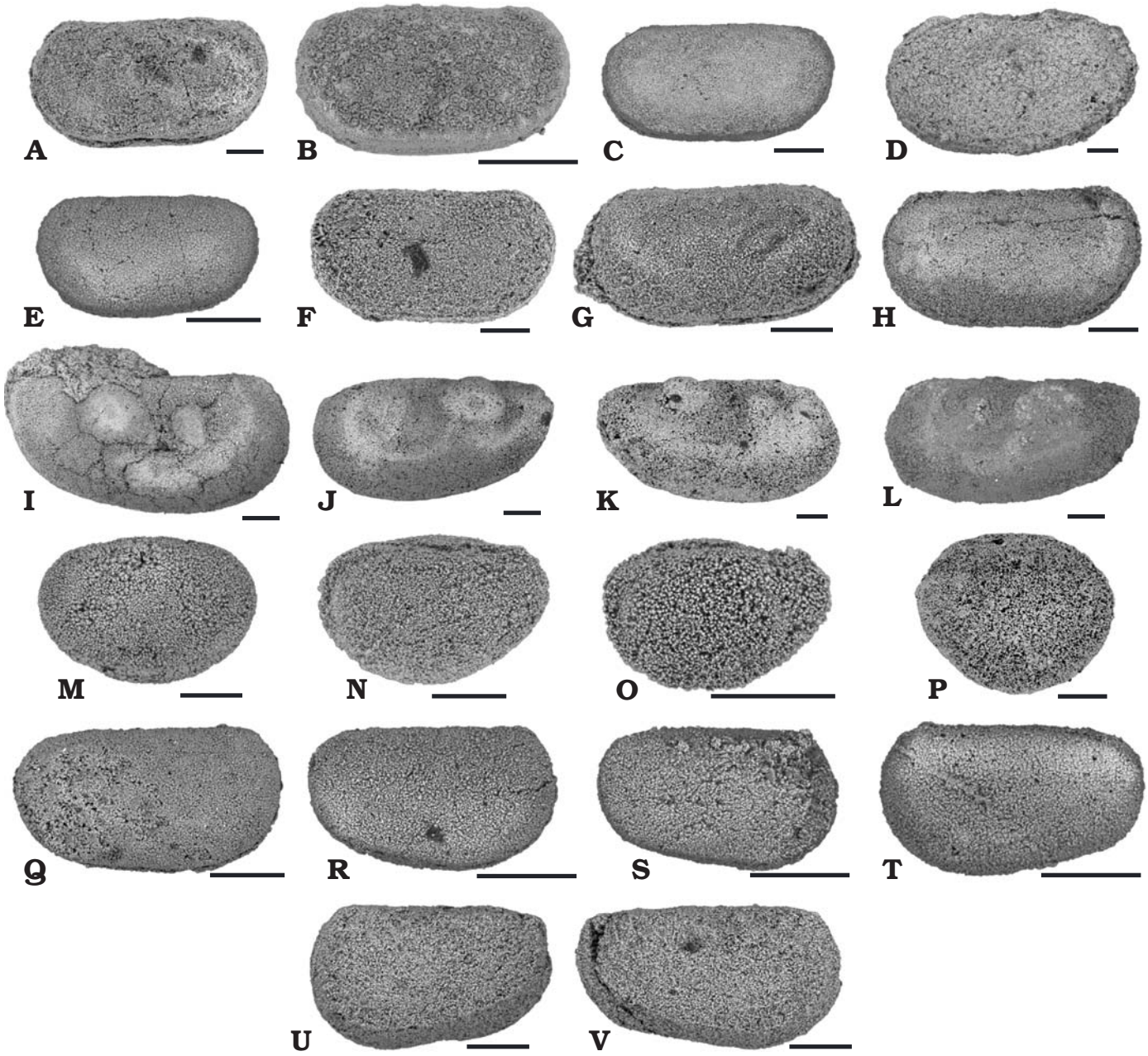

Fig. 4. Ostracods from Bálvány North section, Bükk Mountains, Hungary. Left (A, D–G, N–O) and right (B, M, P–S) lateral views of complete carapaces, external views of a left (J, L, V) and right (I, K, U) valves. **A**–**H**. *Reviya praecurukensis* Forel sp. nov., Changhsingian, Upper Permian. **A**. Holotype, UPMC P6M2742, sample 08BAN47. **B**. Paratype, UPMC P6M2743, sample 08BAN47. **C**. UPMC P6M2744, sample 08BAN47. **D**. UPMC P6M2745, sample 08BAN47. **E**. UPMC P6M2746, sample 08BAN47. **F**. UPMC P6M2747, sample 08BAN47. **G**. UPMC P6M2748, sample 08BAN47. **H**. UPMC P6M2749, sample 08BAN52. **I**–**L**. *Hollinella fengqinglaii* Crasquin sp. nov., Changhsingian, Upper Permian. **I**. Holotype, UPMC P6M2750, sample 08BAN50. **J**. Paratype, UPMC P6M2751, sample 08BAN60. **K**. UPMC P6M2752, sample 08BAN56. **L**. UPMC P6M2753, sample 08BAN60. **M**–**O**. *Samarella meishanella* Forel, 2010, Changhsingian, Upper Permian. **M**. UPMC P6M2754, sample 08BAN56. **N**. UPMC P6M2755, sample 08BAN63. **O**. UPMC P6M2756, sample 08BAN63. **P**. ?*Samarella victori* Crasquin, 2010a, UPMC P6M2757, sample 08BAN56, Changhsingian, Upper Permian. **Q**–**T**. *Shemonaella*? *olempskaella* Forel sp. nov., Changhsingian, Upper Permian. **Q**. Holotype, UPMC P6M2758, sample 08BAN48. **R**. Paratype, UPMC P6M2759, sample 08BAN47. **S**. UPMC P6M2760, sample 08BAN47. **T**. UPMC P6M2761, sample 08BAN47. **U**, **V**. *Reviya curukensis* Crasquin-Soleau, 2004, Griesbachian, Lower Triassic. **U**. UPMC P6M2862, sample 08BAN65. **V**. UPMC P6M2862, sample 08BAN65. Scale bars 100 μm.

Discussion.—*Reviya praecurukensis* sp. nov. differs from *Reviya curukensis* Crasquin-Soleau, 2004 from the Griesbachian (Lower Triassic) of Western Taurus (Turkey) (Crasquin-Soleau et al. 2004a, b) and Meishan GSSP (China) (Crasquin et al. 2010a) by a more quadrangular carapace, a smaller H/L ratio and a straight VB at the RV. *R. praecurukensis* sp. nov. differs from the type species *R. obesa* (Croneis and Gale, 1939), Lower Carboniferous of USA, by the absence of ridges and from *R. mimicus* (Geis, 1932), Lower Carboniferous of USA, by the central position of the

http://dx.doi.org/10.4202/app.2011.0126

pit and the reticulation which is not parallel to free margins. One specimen discovered in the Upper Permian of the Jadar Block in NW Serbia (Crasquin et al. 2010b) was attributed to *Indivisia* cf. *pelikani* Kozur, 1985. This badly preserved specimen could belong to *R. praecurukensis* sp. nov.

Stratigraphic and geographic range.—Bálvány North section, levels 1, 2, 4, samples 08BAN47, 48, 50, 51, 56 (see Fig. 2B), Nagyvisnyó Limestone Formation, Changhsingian, ?Upper Permian of Serbia.

Superfamily Hollinoidea Swartz, 1936

Family Hollinellidae Bless and Jordan, 1971

Genus *Hollinella* Coryell, 1928

Type species: Hollinella dentata Coryell, 1928; Upper Carboniferous of Oklahoma, Texas and Illinois, USA.

Hollinella fengqinglaii Crasquin sp. nov.

Fig. 4I–L.

Etymology: Dedicated to Professor Feng Qinglai (China University of Geosciences, Wuhan, Hubei Province, China).

Type material: Holotype: one right valve, Fig. 4I, UPMC P6M2750, sample 08BAN50. Paratype: one left valve, Fig. 4J, UPMC P6M2751, sample 08BAN60.

Type locality: Bálvány North section, Bükk Mountains, Hungary.

Type horizon: Level 1, Nagyvisnyó Limestone Formation, Changhsingian, Upper Permian.

Material.—7 isolated valves and 2 broken carapaces, samples 08BAN47, 50, 51, 56, 60 (see Fig. 2B), levels 1, 2, 4, 6, Nagyvisnyó Limestone Formation, Bálvány North section, Hungary, Changhsingian, Upper Permian.

Diagnosis.—A species of *Hollinella* with an elongated carapace, a small H/L ratio, a L_1 vertical and thin, bulbous L_2 and L_3, and a well-expressed L_4, which is connected ventrally with L_1.

Dimensions.—L 240–780 μm; H 125–400 μm.

Description.—Carapace elongated (H/L 0.47–0.53); DB long and straight; ACA 110–120°; AB with large radius of curvature, maximum of curvature located at mid-H; VB slightly convex to nearly straight; PB with small radius of curvature, maximum of curvature located high, near to the DB; PCA quite rectangular; carapace flattened along free margins; L_1 thin and quite vertical connected ventrally to L_4 which is always expressed; L_2 bulbous, located at mid-H, it could be subdivided vertically into two nodes connected ventrally; L_3 bulbous and rounded, generally not overpassing DB; maximum of H located behind anterior third of L; ornamentation not observed. Internal features unknown.

Discussion.—The preservation is not very good. All the specimens are represented by isolated valves. Many authors have attributed Lower Triassic specimens of *Hollinella* from South China (Zheng 1976; Wang 1978; Wei 1981; Hao 1992, 1994) and from the Bükk Mountains (Kozur 1985b) to the species *Hollinella tingi* (Patte, 1935). Although these specimens without doubt belong to the genus *Hollinella* they are unlikely *H. tingi* (see discussion in Crasquin-Soleau et al. 2004a). In most cases, the specimens from the Lower Triassic are too corroded to allow a precise attribution. *H. fengqinglaii* sp. nov. described here differs from "*Hollinella tingi*" sensu Wang (1978) and sensu Wei (1981) from the Lower Triassic of South China in its more elongated carapace and absence of nodes on L_3. *H. fengqinglaii* sp. nov. differs from *H. panxiensis* Wang, 1978 from the Upper Permian of South China in its vertical L_1 and rounded L_3 (elongated in *H. panxiensis*). The lateral view of *H. fengqinglaii* sp. nov. is close to *H. derini* Gerry and Honigstein, 1987 from the Upper Permian of Israel (Gerry et al. 1987). This last species has a more elongated L_2 and L_1 is not clearly connected to ventral lobe. The specimen of identified by Kozur (1985a: pl. 13: 3) as *Hollinella tingi* is incomplete and has a larger posterior border and a more bulbous L_3.

Stratigraphic and geographic range.—Bálvány North section, levels 1, 2, 4, 6, samples 08BAN47, 50, 51, 56, 60 (see Fig. 2B), Nagyvisnyó Limestone Formation, Changhsingian, Upper Permian.

Superfamily Paraparchitidea Scott, 1959 emend. Sohn, 1971

Family Paraparchitidae Scott, 1959

Genus *Shemonaella* Sohn, 1971

Type species: *Shemonaella dutroi* Sohn, 1971; Upper Mississippian of Alaska, USA.

Shemonaella? *olempskaella* Forel sp. nov.

Fig. 4Q–T.

Etymology: Dedicated to Professor Ewa Olempska (Institute of Paleobiology PAS, Warsaw, Poland).

Type material: Holotype: one complete carapace, Fig. 4Q, UPMC P6M2758, sample 08BAN48. Paratype: one complete carapace, Fig. 4R, UPMC P6M2759, sample 08BAN47.

Type locality: Bálvány North section, Bükk Mountains, Hungary.

Type horizon: Level 1, Nagyvisnyó Limestone Formation, Changhsingian, Upper Permian.

Material.—6 complete carapaces, samples 08BAN47, 48, 55, 60 (see Fig. 2B), levels 1, 4, 6, Nagyvisnyó Limestone Formation, Bálvány North section, Changhsingian, Upper Permian.

Diagnosis.—A species of *Shemonaella* with long carapace (H/L 0.57) and long straight VB.

Dimensions.—L 240–450 μm; H 140–250 μm.

Description.—Carapace long for the genus (H/L 0.57), DB straight; ACA 125–135°; AB with quite large radius of curvature, maximum at mid-H or little above; VB long and straight (looks curved); the posterior extensions of DB and VB make an angle of 10°; PB with medium radius of curvature and maximum curvature located at 2/3 of H; PCA between 135° and 145°; LV overlaps RV all along free margin; surface smooth. Internal features unknown.

Discussion.—The genus *Shemonaella* is a typically Carboniferous genus and is rare in the Upper Permian. At present,

only one species is reported in the literature (*Shemonaella* sp. 1; Crasquin et al. 2010a: fig. 4K, L). *Shemonaella*? *olempskaella* sp. nov. differs from *Shemonaella* sp. 1 sensu Crasquin et al. 2010a from the Upper Permian of Meishan section in South China in its more elongated and preplete carapace. The closest species in shape is *Shemonaella dutroi* Sohn, 1971 from Lower Carboniferous of Alaska (Sohn 1971). Here the VB is straighter and the carapace longer.

Stratigraphic and geographic range.—Bálvány North section, levels 1, 4, 6, samples 08BAN47, 48, 55, 60 (see Fig. 2B), Nagyvisnyó Limestone Formation, Changhsingian, Upper Permian.

Genus *Langdaia* Wang, 1978

Type species: *Langdaia suboblonga* Wang, 1978; Lower Triassic of Guizhou and Yunnan China.

Langdaia bullabalvanyensis Crasquin sp. nov.

Figs. 5, 6A–G.

2008 *Langdaia suboblonga* Wang, 1978; Crasquin et al. 2008: 238, pl. 1: 3

Etymology: From the occurrence in both Bulla, Italy and Bálvány, Hungary sections.

Type material: Holotype: one complete carapace, Fig. 6A, UPMC P6M2762, sample 05BU19, Bulla section. Paratype: one complete carapace, Fig. 6B, UPMC P6M2763, sample 05BU19, Bulla section.

Type locality: Bulla section, Dolomites, Northern Italy.

Type horizon: Mazzin Member, Werfen Formation, Griesbachian, Lower Triassic, Bulla section, Northern Italy (Crasquin et al. 2008).

Material.—11 complete and 1 broken carapaces, Mazzin Member, Werfen Formation, Bulla section, Northern Italy (Crasquin et al. 2008); sample 08BAN67 (see Fig. 2B), level 8, Gerennavár Limestone Formation, Bálvány North section, Griesbachian, Lower Triassic.

Diagnosis.—A species of *Langdaia* with large AB, long straight VB, S_2 very faint.

Dimensions.—L 250–500 μm; H 150–320 μm (see Fig. 5).

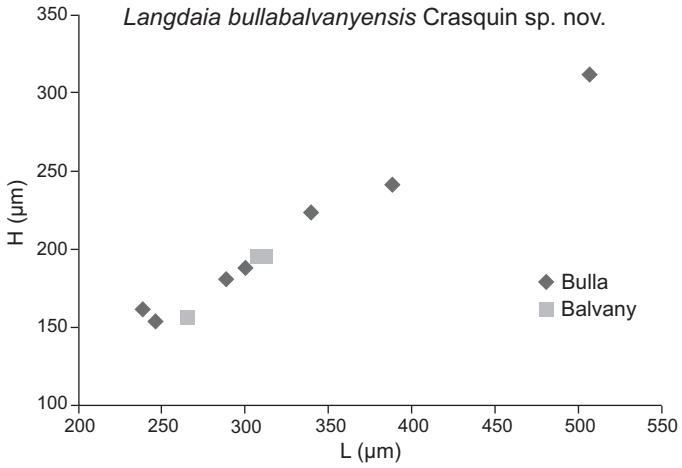

Fig. 5. Height/length diagram of *Langdaia bullabalvanyensis* Crasquin sp. nov.

Description.—Carapace with long straight DB; ACA 140–150°; AB with large radius of curvature, maximum located at mid-H; VB long, straight in the youngest specimens, a little convex in the adults; PB with quite small radius of curvature, maximum located at or a little below mid-H; DB and VB converge towards the posterior end with an angle of 15° at the instars and 25° at the adults; PCA 150°; S_2 very faint, visible on adult specimens located at mid-H and mid-L; RV overlaps LV all along free margins; surface smooth. Internal features unknown.

Discussion.—Specimens attributed to *Langdaia suboblonga* Wang, 1978 were found in the Lower Triassic of Northern Italy (Bulla section; Crasquin et al. 2008). This specific attribution is wrong. *Langdaia suboblonga* Wang, 1978 from lowermost Triassic of South China (Wang 1978; Crasquin and Kershaw 2005) has a deeper S_2, a more obtuse ACA and a PB with larger radius of curvature. All the other species of the genus are more quadrangular.

Stratigraphic and geographic range.—Mazzin Member, Werfen Formation, Bulla section, Northern Italy, Griesbachian (Crasquin et al. 2008); Bálvány North section, level 8, sample 08BAN67 (see Fig. 2B), Gerennavár Limestone Formation, Griesbachian, Lower Triassic.

Order Podocopida Müller, 1894

Suborder Podocopina Sars, 1866

Superfamily Bairdioidea Sars, 1887

Family Bairdiidae Sars, 1887

Genus *Bairdia* McCoy, 1844

Type species: *Bairdia curta* McCoy, 1844; Carboniferous, Ireland.

Bairdia anisongae Forel sp. nov.

Figs. 6N–P, 7.

Etymology: Dedicated to Dr. Anisong Chitnarin (Suranaree University of Technology, Nakhon Ratchasima, Thailand).

Type material: Holotype: one complete carapace, Fig. 6N, UPMC P6M2774, sample 08BAN55. Paratype: one complete carapace, Fig. 6O, UPMC P6M2775, sample 08BAN62.

Type locality: Bálvány North section, Bükk Mountains, Hungary.

Type horizon: Level 4, Nagyvisnyó Limestone Formation, Changhsingian, Upper Permian.

Material.—Three complete and four broken carapaces, samples 08BAN47, 55 and 62 (see Fig. 2B), levels 1, 4, 8, Nagyvisnyó and Gerennavár Limestone Formations, Bálvány North section, Hungary, Changhsingian to Griesbachian, Upper Permian–Lower Triassic.

Diagnosis.—A species of *Bairdia* with straight PDB, DB, and ADB, with narrow AB and almost parallel AVB and PDB.

Dimensions.—L 210–325 μm; H 120–200 μm (see Fig. 7).

Description.—Carapace quite high (H/L 0.57–0.63), with straight DB, PDB, and ADB at both valves; DB steeply inclined backwards; AB with small radius of curvature and maximum of convexity located high (above mid-H); AVB

http://dx.doi.org/10.4202/app.2011.0126

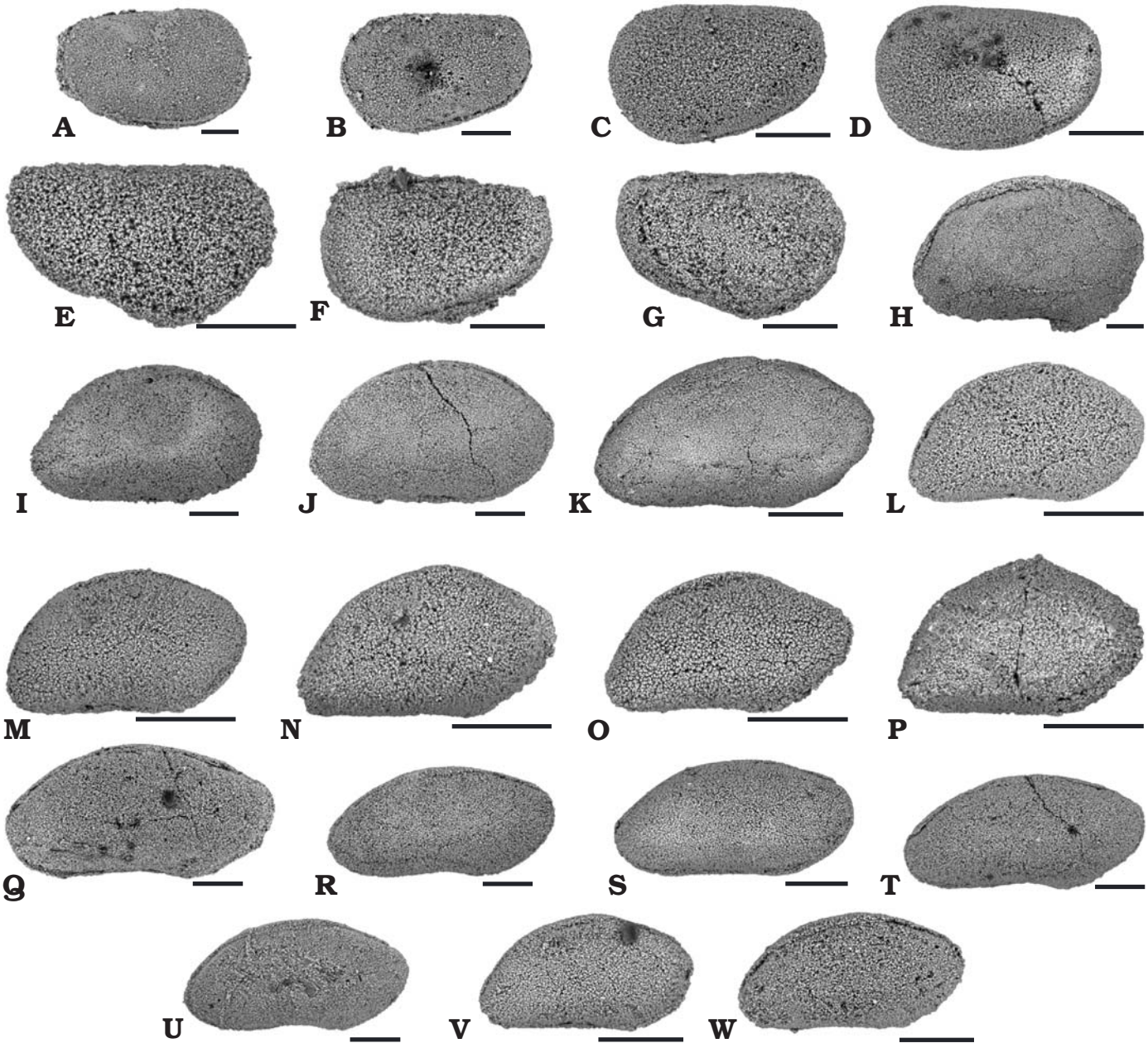

Fig. 6. Ostracods from Bálvány North section, Hungary (except A–D from Bulla section, Northern Italy). Right (A, E, G–W) and left (B, C, D, F) lateral views of complete carapaces. **A**–**G**. *Langdaia bullabalvanyensis* Crasquin sp. nov., Griesbachian, Lower Triassic. **A**. Holotype, UPMC P6M2762, sample 05BU19. **B**. Paratype, UPMC P6M2763, sample 05BU19. **C**. UPMC P6M2232, sample 05BU19. **D**. UPMC P6M2764, sample 05BU19. **E**. UPMC P6M2765, sample 08BAN67. **F**. UPMC P6M2766, sample 08BAN67. **G**. UPMC P6M2767, sample 08BAN67. **H**, **I**. *Bairdia baudini* nom. nov. **H**. UPMC P6M2785, sample 08BAN48, Changhsingian, Upper Permian. **I**. UPMC P6M2786, sample 08BAN61, Griesbachian, Lower Triassic. **J**–**M**. *Bairdia wailiensis* Crasquin-Soleau, 2006, Griesbachian, Lower Triassic. **J**. UPMC P6M2770, sample 08BAN62. **K**. UPMC P6M2771, sample 08BAN47. **L**. UPMC P6M2772, sample 08BAN62. **M**. UPMC P6M2773, sample 08BAN62. **N**–**P**. *Bairdia anisongae* Forel sp. nov. **N**. Holotype, UPMC P6M2774, sample 08BAN55, Changhsingian, Upper Permian. **O**. Paratype, UPMC P6M2775, sample 08BAN62, Grisbachian, Lower Triassic. **P**. UPMC P6M2776, sample 08BAN47, Changhsingian, Upper Permian. **Q**–**U**. *Bairdia davehornei* Forel sp. nov., Griesbachian, Lower Triassic. **Q**. Holotype, UPMC P6M2777, sample 08BAN61. **R**. Paratype, UPMC P6M2778, sample 08BAN62. **S**. UPMC P6M2779, sample 08BAN62. **T**. UPMC P6M2780, sample 08BAN62. **U**. UPMC P6M2781, sample 08BAN62. **V**, **W**. *Bairdia* cf. *Bairdia davehornei* Forel sp. nov., Griesbachian, Lower Triassic. **V**. UPMC P6M2782, sample 08BAN62. **W**. UPMC P6M2783, sample 08BAN61. Scale bars 100 μm.

straight and long, almost parallel to PDB; VB long and quite straight at both valves; PB with small radius of curvature with maximum of convexity located low (lower than 1/5th of H); PDB straight and long at both valves; Hmax located a little in front of mid-L; LV overlaps RV very faintly all around the carapace with a maximum at DB, carapace biconvex and thin in dorsal view. Internal features unknown.

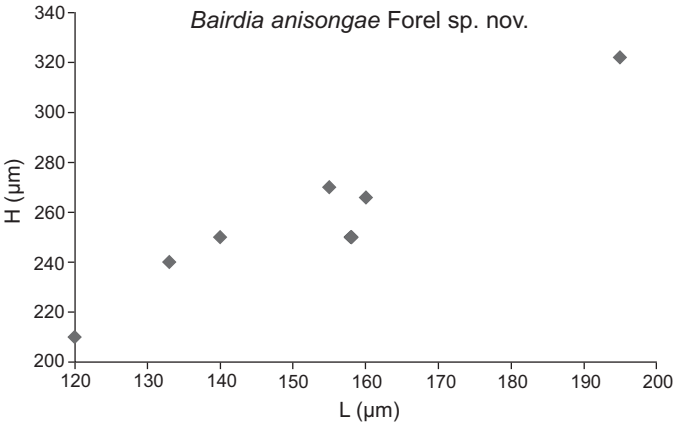

Fig. 7. Height/length diagram of *Bairdia anisongae* Forel sp. nov.

Discussion.—*Bairdia anisongae* sp. nov. shows the same angularity between dorsal parts (PDB/DB/ADB) as *Bairdia wushunbaoi* Crasquin, 2010 and *Bairdia paussi* Crasquin, 2010 both from Changhsingian of Meishan section (Crasquin et al. 2010a). In *B. wushunbaoi* the AB is narrower and its maximum of curvature is located higher. *B. paussi* has a more elongated carapace with a less strongly inclined DB. *Bairdia anisongae* sp. nov. differs from *B. wailiensis* Crasquin-Soleau, 2006 from the Lower Triassic of Guangxi (Crasquin-Soleau et al. 2006) (see Fig. 5J–M) in its more distinct dorsal parts, its more tapering PB and the smaller radius of curvature of AB.

Stratigraphic and geographic range.—Bálvány North section, levels 1 to 8, samples 08BAN47, 55 and 62 (see Fig. 2B), Nagyvisnyó and Gerennavár Limestone Formations, Changhsingian to Griesbachian, Upper Permian to Lower Triassic.

Bairdia davehornei Forel sp. nov.

Figs. 6Q–U, 8.

Etymology: Dedicated to Professor David J. Horne (Queen Mary University, London).

Type material: Holotype: one complete carapace, Fig. 6Q, UPMC P6M2777, sample 08BAN61. Paratype: one complete carapace, Fig. 6R, UPMC P6M2778, sample 08BAN62.

Type locality: Bálvány North section, Bükk Mountains, Hungary.

Type horizon: Level 7, Gerennavár Limestone Formation, Changhsingian, Upper Permian.

Material.—32 complete and 2 broken carapaces, samples 08BAN47, 61 and 62 (see Fig. 2B), levels 1, 7, 8, Nagyvisnyó and Gerennavár Limestone Formations, Bálvány North section, Hungary, Changhsingian to Griesbachian, Upper Permian–Lower Triassic.

Diagnosis.—A species of *Bairdia* with an elongated carapace (L/H = 2) with a truncated AVB, regularly arched dorsal parts, and a rounded PB with the maximum of curvature at lower 1/3rd of H.

Dimensions.—L 290–560 µm; H 141–275 µm (see Fig. 8).

Description.—Carapace elongated (L = 2H), DB, PDB, and ADB regularly arched at LV; DB, PDB, and ADB quite straight at RV; AB with small radius of curvature, with maximum of curvature located above mid-H; AVB truncated; VB concave, particularly at RV; PB rounded with large radius of curvature, maximum of curvature located at the lower 1/3 of H; typical bairdian beak visible only on some specimens; LV overlaps RV slightly all around the carapace with maximum at DB; Hmax located near mid-L. Internal features unknown.

Discussion.—*Bairdia davehornei* sp. nov. could be compared to *Bairdia fangnianqiaoi* Crasquin, 2010 from the Griesbachian Meishan section (China; Crasquin et al. 2010a). The latter species has a more slender PB and a more elongated carapace in lateral view. *Cryptobairdia heshanenis* Chen, 2002 (Wuchiapingian of Matan and Pinding section, China; Shi and Chen 2002) is also close to *Bairdia davehornei* sp. nov. but has a more distinct flattened and a larger AB. *Bairdia davehornei* sp. nov. differs from *Bairdia*? *kemerensis* from the Griesbachian of Turkey (Crasquin-Soleau et al. 2004b) in its shorter DB and smaller AB.

Stratigraphic and geographic range.—Bálvány North section, levels 1 to 8, samples 08BAN47, 61 and 62 (see Fig. 2B), Nagyvisnyó and Gerennavár Limestone Formations, Changhsingian–Griesbachian, Upper Permian–Lower Triassic.

Bairdia baudini Crasquin nom. nov.

Fig. 6H, I.

Non 1978 *Bairdia subsymmetrica* Sun sp. nov.; Guan et al. 1978: 152, pl. 39 :10.

1987 *Silenites subsymmetrica* Shi, 1987; Shi and Chen 1987: 63, pl. 15: 4–11.

2004 *Bairdia subsymmetrica* (Shi, 1987); Crasquin-Soleau et al. 2004b: 285, pl. 2: 7–12.

2004 *Bairdia subsymmetrica* (Shi, 1987); Crasquin-Soleau et al. 2004a: 71, pl. 1: 13–14.

Etymology: Dedicated to Professor François Baudin (UPMC, Paris, France).

Discussion.—This species was described by Shi (Shi and Chen 1987) from the uppermost Permian (Changhsingian) of Meishan. It was attributed to the genus *Bairdia* by Crasquin-Soleau et al. (2004a, b). The species name *Bairdia subsym-*

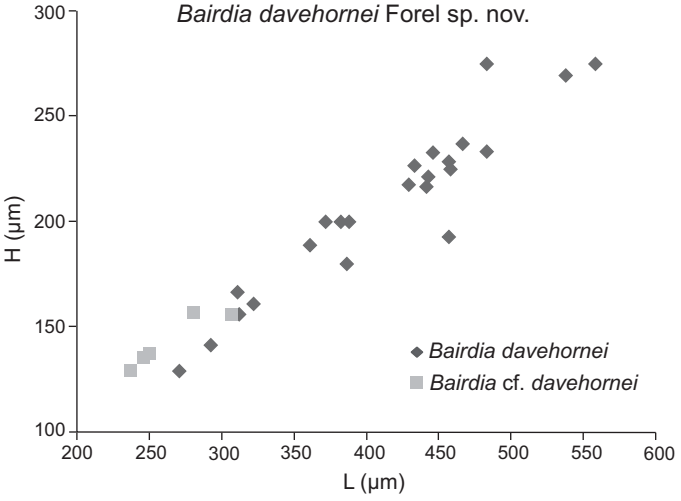

Fig. 8. Height/length diagram of *Bairdia davehornei* Forel sp. nov.

http://dx.doi.org/10.4202/app.2011.0126

metrica is already used for a species described by Sun (in Guan et al. 1978) from western Hubei Province, Qixia Formation, Guadalupian. Therefore, a new specific name is given.

Stratigraphic and geographic range.—Meishan section, South China, Upper Changhsingian, Upper Permian (Shi and Chen 1987); Çürük Dağ section Western Taurus, Turkey, Griesbachian, Lower Triassic (Crasquin-Soleau et al. 2004a, b); samples 08BAN48 and 62 (see Fig. 2B), levels 1, 8, Nagyvisnyó and Gerennavár Limestone Formations, Bálvány North section, Changhsingian to Griesbachian, Upper Permian–Lower Triassic.

Family Acratiidae Gründel, 1962

Genus *Acratia* Delo, 1930

Type species: *Acratia typica* Delo, 1930; Upper Carboniferous of Texas, USA.

Acratia? *jeanvannieri* Forel sp. nov.

Figs. 9, 10A–J.

Etymology: Dedicated to Dr. Jean Vannier (CNRS-Lyon 1 University, Lyon, France).

Type material: Holotype: one complete carapace, Fig. 10A, UPMC P6M2803, sample 08BAN61. Paratype: one complete carapace, Fig. 10B, UPMC P6M2804, sample 08BAN63.

Type locality: Bálvány North section, Bükk Mountains, Hungary.

Type horizon: Level 7, Gerennavár Limestone Formation, Griesbachian (Lower Triassic).

Material.—139 complete and 12 broken carapaces, samples 08BAN52?, 54?, 56, 61, 62, 64, 65, 67, and 69 (see Fig. 2B), levels 3?, 4, 7, 8, Nagyvisnyó and Gerennavár Limestone Formations, Changhsingian to Griesbachian, Upper Permian– Lower Triassic.

Diagnosis.—A species of *Acratia* with a compact carapace, poorly slender extremities and a poorly expressed acratian beak.

Dimensions.—L 163–708 μm; H 102–325 μm (101 mesured specimens; see Fig. 9).

Description.—Compact carapace; DB long, straight at RV, straight to gently convex at LV; ADB convex in LV, straight to gently concave at RV, AB with rather large radius of curvature for the genus, with maximum of curvature located around lower 1/3rd of H; acratian beak poorly expressed in RV, absent in LV; VB straight to gently convex at LV, gently concave at RV; PVB rectangular particularly at RV; LV overlaps RV all around the carapace with maximum at ADB and PDB; AB flattened laterally at some specimens; Hmax located behind 2/3rd of L. Internal features unknown.

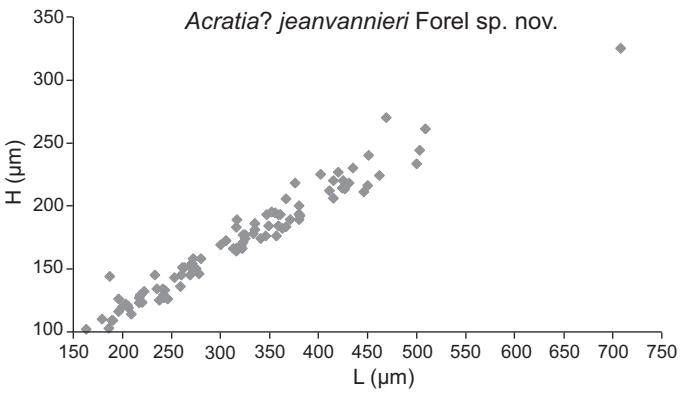

Fig. 9. Height/length diagram of *Acratia*? *jeanvannieri* Forel sp. nov.

Discussion.—The species displays a significant intraspecific variation with regard to the carapace outline. The very small forms show a broader AB and a higher H/L ratio compared to larger specimens. The doubt on generic attribution comes from the fact that the acratian beak is poorly expressed. The internal characters should be seen to be sure.

Acratia? *jeanvannieri* sp. nov. is comparable to *Acratia symmetrica* Hao, 1992 from the Lower Triassic of Guizhou Province (South China; Hao 1992). The DB of *A.*? *jeanvannieri* sp. nov. is straighter, the extremities are not slender and the H/L ratio is higher (*A. symmetrica*: 0.44, *A.*? *jeanvannieri* sp. nov.: 0.55).

Stratigraphic and geographic range.—Bálvány North section, levels 3? to 8, samples 08BAN52?, 54?, 56, 61, 62, 64, 65, 67, and 69 (see Fig. 2B), Nagyvisnyó and Gerennavár Limestone Formations, Changhsingian to Griesbachian, Upper Permian to Lower Triassic.

Acratia nagyvisnyoensis Forel sp. nov.

Fig. 10K–O.

Etymology: In reference to the occurrence of the species in the Nagyvisnyó Limestone Formation.

Type material: Holotype: one complete carapace, Fig. 10K, UPMC P6M2813, sample 08BAN47. Paratype: one complete carapace, Fig. 10L, UPMC P6M2814, sample 08BAN47.

Type locality: Bálvány North section, Bükk Mountains, Hungary.

Type horizon: Level 1, Nagyvisnyó Limestone Formation, Changhsingian (Upper Permian).

Material.—7 complete and 5 broken carapaces, samples 08BAN47, 48, 50, 53, and 54 (see Fig. 2B), levels 1, 3, 4, Nagyvisnyó Limestone Formation, Bálvány North section, Hungary, Changhsingian (Upper Permian).

Diagnosis.—A species of *Acratia* with laterally flattened extremities, a *Bairdia*-type PB, and a fairly symmetrical carapace in lateral view with Hmax located at midL.

Dimensions.—L 550–610 μm; H 300–310 μm.

Description.—Lateral carapace outline subsymmetrical, Hmax located at midL; DB regularly arched at both valves; ADB and PDB quite straight to gently convex; AB with small radius of curvature, quite vertical; anterior acratian beak poorly expressed; VB convex at LV, straight to gently convex at RV; *Bairdia*-type PB, with maximum of curvature located at lower 1/3rd of H; LV overlaps RV all around the carapace with maximum at VB; both extremities laterally flattened. Internal features unknown.

Discussion.—*Acratia nagyvisnyoensis* sp. nov. is similar to *Acratia subfusiformis* Wang, 1978 from Wuchiapingian and Changhsingian of Southern China: Guizhou and Yunnan

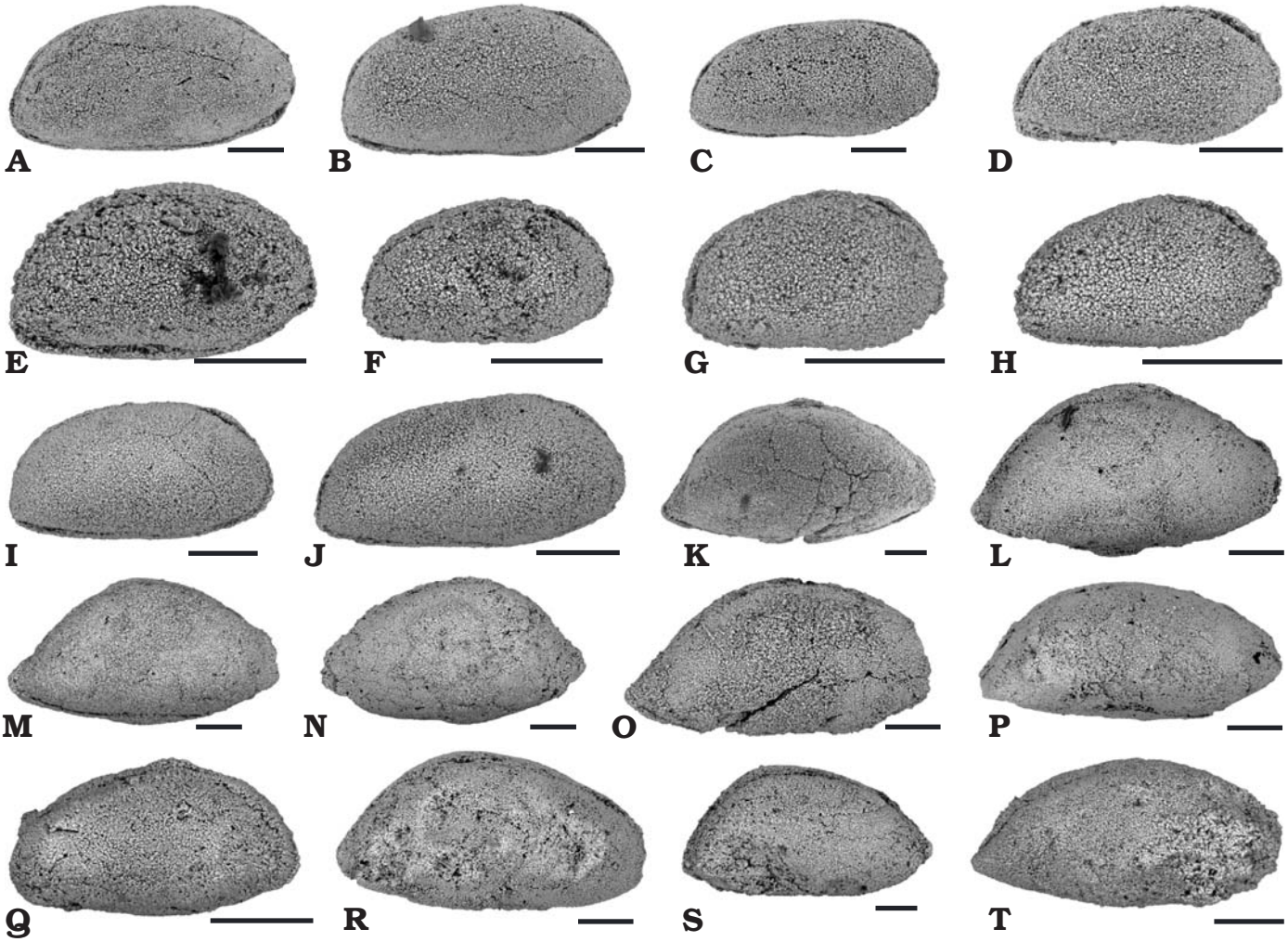

Fig. 10. Ostracods from Bálvány North section, Bükk Mountains, Hungary. Right lateral views of complete carapaces. **A**–**J**. *Acratia*? *jeanvannieri* Forel sp. nov., Griesbachian, Lower Triassic. **A**. Holotype, UPMC P6M2803, sample 08BAN61. **B**. Paratype, UPMC P6M2804, sample 08BAN63. **C**. UPMC P6M2805, sample 08BAN63. **D**. UPMC P6M2806, sample 08BAN63. **E**. UPMC P6M2807, sample 08BAN61. **F**. UPMC P6M2808, sample 08BAN61. **G**. UPMC P6M2809, sample 08BAN63. **H**. UPMC P6M2810, sample 08BAN63. **I**. UPMC P6M2811, sample 08BAN62. **J**. UPMC P6M2812, sample 08BAN62. **K**–**O**. *Acratia nagyvisnyoensis* Forel sp. nov., Changhsingian, Upper Permian. **K**. Holotype, UPMC P6M2813, sample 08BAN47. **L**. Paratype, UPMC P6M2814, sample 08BAN47. **M**. UPMC P6M2815, sample 08BAN47. **N**. UPMC P6M2816, sample 08BAN47. **O**. UPMC P6M2817, sample 08BAN54. **P**, **T**. *Acratia* sp. A, Changhsingian, Upper Permian. **P**. UPMC P6M2818, sample 08BAN47. **T**. UPMC P6M2819, sample 08BAN47. **Q**. *Acratia* sp. B, Changhsingian, Upper Permian. UPMC P6M2820, sample 08BAN47. **R**, **S**. *Acratia* sp. C, Changhsingian, Upper Permian. **R**. UPMC P6M2821, sample 08BAN50. **S**. UPMC P6M2822, sample 08BAN52. Scale bars 100 μm.

(Wang 1978), Guangxi (Shi and Chen 2002), and Meishan GSSP section, Zhejiang (Crasquin et al. 2010a). The PB are very similar in the two species. In *A. nagyvisnyoensis* sp. nov., the maximum of curvature is located lower, the Hmax is located more posteriorly and the VB is more convex. *A. nagyvisnyoensis* sp. nov. is also close to *Acratia zhongyingensis* Wang, 1978 from Wuchiapingian and Changhsingian of Southern China: Guizhou and Yunnan (Wang 1978), Guangxi (Shi and Chen 2002), and Meishan GSSP section, Zhejiang (Crasquin et al. 2010a), and from the Changhsingian of Bulla section, Italy (Crasquin et al. 2008). Both species have laterally flattened extremities. In *A. nagyvisnyoensis* sp. nov. the DB is more convex, more symmetrical in lateral view and shows a greater overlap.

Stratigraphic and geographic range.—Bálvány North section, levels 1, 3, 4, samples 08BAN47, 50, 53, and 54 (see Fig. 2B), Nagyvisnyó Limestone Formation, Changhsingian, Upper Permian.

Genus *Liuzhinia* Zheng, 1976

Type species: *Liuzhinia subovata* Zheng, 1976; Anisian (Middle Triassic) of Guizhou Province, China.

Liuzhinia venninae Forel sp. nov.

Figs. 11, 12A–K.

Etymology: Dedicated to Professor Emmanuelle Vennin (University of Burgundy, Dijon, France).

Type material: Holotype: one complete carapace, Fig. 12A, UPMC

http://dx.doi.org/10.4202/app.2011.0126

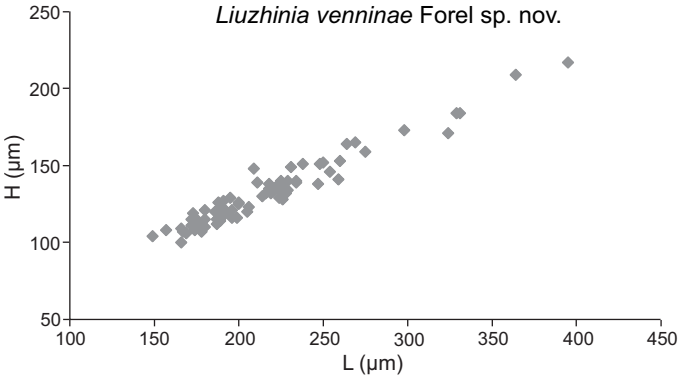

Fig. 11. Height/length diagram of *Liuzhinia venninae* Forel sp. nov.

P6M2842, sample 08BAN63. Paratype: one complete carapace, Fig. 12D, UPMC P6M2845, sample 08BAN61.

Type locality: Bálvány North section, Bükk Mountains, Hungary.

Type horizon: Level 8, Gerennavár Limestone Formation, Griesbachian, Lower Triassic.

Material.—128 complete and 8 broken carapaces, samples 08BAN61, 62, 63, 67, and 69 (see Fig. 2B), levels 7, 8, Gerennavár Limestone Formation, Bálvány North section, Hungary, Griesbachian, Lower Triassic.

Diagnosis.—A species of *Liuzhinia* with small carapace with a long, almost straight DB; which is strongly biconvex in dorsal view.

Dimensions.—L 550–610 µm; H 300–310 µm (see Fig. 11).

Description.—Carapace small and strongly convex in dorsal view; DB long and straight; AB with quite large radius of curvature for the genus, maximum of curvature located at mid-H; VB long and straight at LV, gently concave at RV; PB with small radius of curvature (pointed in RV), dorsal part straight at RV; LV slightly overlaps RV on free margin. Internal features unknown.

Discussion.—*Liuzhinia venninae* sp. nov. is close to *Liuzhinia antalyaensis* Crasquin-Soleau, 2004 from the Griesbachian of Western Taurus (Turkey; Crasquin-Soleau et al. 2004b) and Guangxi (South China; Crasquin-Soleau et al. 2006). Here, the DB is longer, the AB has a larger radius of curvature, the carapace is smaller and more inflated in dorsal view. *Liuzhinia venninae* sp. nov. differs from *Liuzhinia praeantalyaensis* Forel, 2010 from the Upper Changhsingian of Meishan GSSP (South China; Crasquin et al. 2010a) by the absence of a lateral compression at the extremities, a more developed valve overlap and a higher H/L ratio.

Stratigraphic and geographic range.—Bálvány North section, level 8, samples 08BAN61, 62, 63, 67, and 69 (see Fig. 2B), Gerennavár Limestone Formation, Griesbachian, Lower Triassic.

Liuzhinia bankutensis Forel sp. nov.

Fig. 12L–R.

Etymology: In reference to the tourist center of Bánkút, situated near to the Bálvány North section.

Type material: Holotype: one complete carapace, Fig. 12L, UPMC P6M2853, sample 08BAN67. Paratype: one complete carapace, Fig. 12M, UPMC P6M2854, sample 08BAN69.

Type locality: Bálvány North section, Bükk Mountains, Hungary.

Type horizon: Level 8, Gerennavár Limestone Formation, Griesbachian, Lower Triassic.

Material.—14 complete and 2 broken carapaces, samples 08BAN47, 53, 63, 65, 67, and 69 (see Fig. 2B), levels 1 3, 8, Nagyvisnyó and Gerennavár Limestone Formations, Bálvány North section, Hungary, Changhsingian to Griesbachian, Upper Permian–Lower Triassic.

Diagnosis.—A species of *Liuzhinia* with a rounded PB and a long and straight DB and VB in both valves.

Dimensions.—L 195–290 µm; H 105–150 µm.

Description.—Carapace elongated in lateral view (H/L 0.53); DB long (between 50% and 65% of L) and straight; AB quite hemicircular with small radius of curvature for the genus; VB long and straight in both valves; DB and VB converge at an angle of 15–18° towards the anterior end; PB with quite large radius of curvature (particularly in small specimens); LV overlaps RV all around the carapace; surface smooth; significant intraspecific variation with regard to radius of curvature of PB in larval stages.

Discussion.—*Liuzhinia bankutensis* sp. nov. could be compared to *Liuzhinia venninae* sp. nov. (see above), which has a shorter carapace, an AB with larger radius of curvature and a more strongly tapering PB. *Liuzhinia praeantalyaensis* Forel, 2010 from Changhsingian of South China (Yi 2004; Crasquin et al. 2010a) has a PB with smaller radius of curvature and laterally compressed extremities. *Liuzhinia antalyaensis* Crasquin-Soleau, 2004 from the Griesbachian of Taurus (Turkey, Crasquin-Soleau et al. 2004b) and South China (Guangxi, Crasquin-Soleau et al. 2006) is also close to *Liuzhinia bankutensis* sp. nov., which has a PB more rounded, a longer DB and a straight VB in RV.

Stratigraphic and geographic range.—Bálvány North section, levels 1, 3, 8, samples 08BAN47, 53, 63, 65, 67, and 69 (see Fig. 2B), Nagyvisnyó and Gerennavár Limestone Formations, Changhsingian to Griesbachian, Upper Permian–Lower Triassic.

Suborder Metacopina Sylvester-Bradley, 1961

Superfamily Healdioidea Harlton, 1933

Family Healdiidae Harlton, 1933

Genus *Hungarella* Mehés, 1911

Type species: *Hungarella problematica* Méhes, 1911; Upper Triassic of Hungary.

Hungarella gerennavarensis Crasquin sp. nov.

Figs. 13, 15M–P.

Etymology: In reference to the occurrence of the species in the Gerennavár Limestone Formation.

Type material: Holotype: one complete carapace, Fig. 14M, UPMC P6M2875, sample 08BAN62. Paratype: one complete carapace, Fig. 14N, UPMC P6M2876, sample 08BAN67.

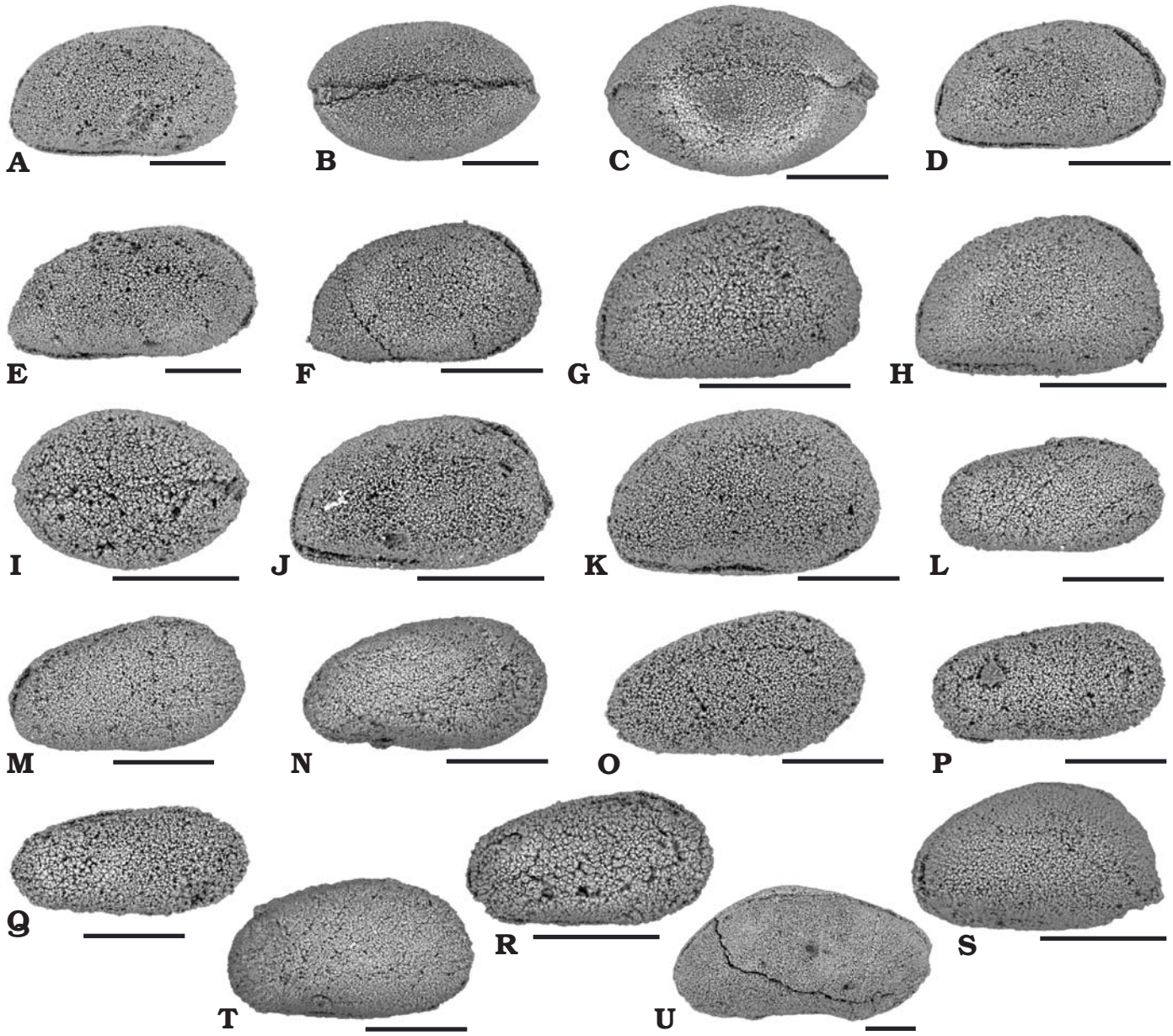

Fig. 12. Ostracods from Bálvány North section, Bükk Mountains, Hungary. Right lateral (A, D–H, J–U) and dorsal (B, C, I) views of complete carapaces. **A**–**K**. *Liuzhinia venninae* Forel sp. nov., Griesbachian, Lower Triassic. **A**. Holotype, UPMC P6M2842, sample 08BAN63. **B**. UPMC P6M2843, sample 08BAN63. **C**. Dorsal view of a complete carapace, UPMC P6M2844, sample 08BAN63. **D**. Paratype, UPMC P6M2845, sample 08BAN61. **E**. UPMC P6M2846, sample 08BAN63. **F**. UPMC P6M2847, sample 08BAN63. **G**. UPMC P6M2848, sample 08BAN62. **H**. UPMC P6M2849, sample 08BAN61. **I**. UPMC P6M2850, sample 08BAN63. **J**. UPMC P6M2851, sample 08BAN61. **K**. UPMC P6M2852, sample 08BAN63. **L**–**R**. *Liuzhinia bankutensis* Forel sp. nov. **L**. Holotype, UPMC P6M2853, sample 08BAN67, Giresbachian, Lower Triassic. **M**. Paratype, UPMC P6M2854, sample 08BAN69, Griesbachian, Lower Triassic. **N**. UPMC P6M2915, sample 08BAN47, Changhsingian, Upper Permian. **O**. UPMC P6M2855, sample 08BAN63, Giresbachian, Lower Triassic. **P**. UPMC P6M2856, sample 08BAN67, Griesbachian,Lower Triassic. **Q**. UPMC P6M2857, sample 08BAN67, Griesbachian, Lower Triassic. **R**. UPMC P6M2858, sample 08BAN67, Griesbachian, Lower Triassic. **S**. *Liuzhinia* sp. A. UPMC P6M2859, sample 08BAN62, Griesbachian, Lower Triassic. **T**. *Liuzhinia* sp. B. UPMC P6M2768, sample 08BAN47, Changhsingian, Upper Permian. **U**. *Bairdiacypris fornicata* Shi, 1982. UPMC P6M2860, sample 08BAN62, Griesbachian, Lower Triassic. Scale bars 100 μm.

Type locality: Bálvány North section, Bükk Mountains, Hungary.

Type horizon: Level 8, Gerennavár Limestone Formation, Griesbachian, Lower Triassic.

Material.—5 complete and 1 broken carapaces, samples 08BAN62, 63, 64, and 67 (see Fig. 2B), level 8, Gerennavár Limestone Formation, Bálvány North section, Hungary, Griesbachian, Lower Triassic.

Diagnosis.—A species of *Hungarella* with a high vertical PB, Hmax located behind mid-L.

Dimensions.—L 250–560 μm; H 150–300 μm (see Fig. 13).

Description.—Carapace quite short (H/L = 0.60); PB quite vertical with angular contact with VB; VB convex to straight at RV, concave at LV; dorsal parts of LV more or

http://dx.doi.org/10.4202/app.2011.0126

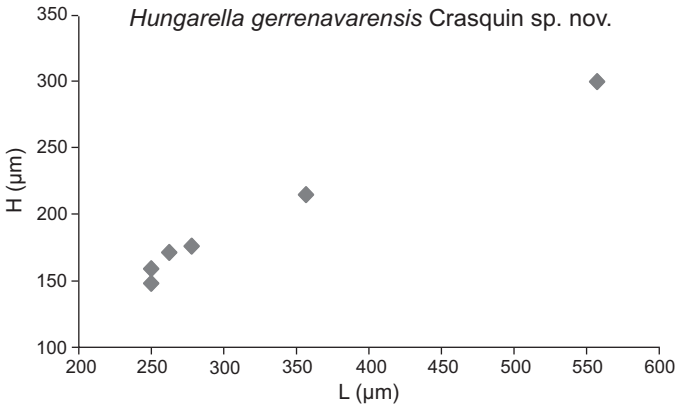

Fig. 13. Height/length diagram of *Hungarella gerennavarensis* Crasquin sp. nov.

less regularly rounded, DB and PDB in continuity, ADB nearly straight; dorsal margin of RV clearly differentiated into straight PDB, DB and ADB; AB regularly arched with maximum of curvature located between lower 1/3 and 1/2 of H; Hmax located behind mid-L; LV slightly overlaps RV all around the carapace. Internal features unknown.

Discussion.—*Hungarella gerennavarensis* sp. nov. differs from "*Healdia*" sp. A from Griesbachian of Guangxi (Crasquin-Soleau et al. 2006) in its more vertical PB, from *Hungarella tulongensis* Crasquin, 2011 from Spathian to Anisian of South Tibet (Forel and Crasquin 2011a) in the more posterior position of Hmax and the lack of a lateral compression at the AB.

Stratigraphic and geographic range.—Bálvány North section, level 8, samples 08BAN62, 63, 64, and 67 (see Fig. 2B), Gerennavár Limestone Formation, Griesbachian, Lower Triassic.

Family Bairdiocyprididae Shaver, 1961

Genus *Cytherellina* Jones and Holl, 1869

Type species: *Beyrichia siliqua* Jones, 1855; Silurian of England.

Cytherellina? *magyarorszagensis* Forel sp. nov.

Figs. 14, 15B–J.

2011 *Bythocypris* cf *Bythocypris* sp. B sensu Bolz, 1971; Forel and Crasquin 2011a: pl. 5: 8, table 1.

Etymology: From Hungarian Magyarország, Hungary.

Type material: Holotype: one complete carapace, Fig. 15B, UPMC P6M2864, sample 08BAN63. Paratype: one complete carapace, Fig. 15C, UPMC P6M2865, sample 08BAN61.

Type locality: Bálvány North section, Bükk Mountains, Hungary.

Type horizon: Level 8, Gerennavár Limestone Formation, Griesbachian, Lower Triassic.

Material.—23 complete carapaces, samples 08BAN61, 62, 63, and 64? (see Fig. 2B), levels 7, 8, Gerennavár Limestone Formation, Bálvány North section, Hungary, Griesbachian, Lower Triassic; Tulong section, Tibet, Anisian, Middle Triassic (Forel and Crasquin 2011a; Forel et al. 2011).

Diagnosis.—A species of *Cytherellina*? with a high and vertical PB and Hmax located in front of mid-L.

Dimensions.—L 200–550 µm; H 110–320 µm (see Fig. 14).

Description.—Carapace short (H/L 0.60); PB almost vertical with angular contact with VB; VB straight to gently concave at both valves; dorsal parts of LV more or less regularly rounded, DB and PDB in continuity, ADB nearly straight; dorsal parts of RV clearly distinct, PDB, DB and ADB long and straight; AB regularly arched with maximum of curvature located at mid-H; at adult specimens AB could be laterally flattened; Hmax located in front of mid-L; LV slightly overlaps RV all around the carapace with maximum at PDB. Internal features unknown.

Discussion.—*Cytherellina*? *magyarorszagensis* sp. nov. is comparable to *Pseudobythocypris guiqianensis* Yuan, 2009 from the Upper Changhsingian of South China (Yuan et al. 2007, 2009). The latter species is longer and the maximum of convexity of the AB is located lower. Great confusion exists in the systematics of the smooth shelled bairdiid genera of the Upper Permian–Lower Triassic. A full revision of all these forms is necessary.

Stratigraphic and geographic range.—Tulong section, Tibet, Anisian, Middle Triassic (Forel and Crasquin 2011a; Forel et al. 2011); Bálvány North section, levels 7, 8, samples 08BAN61, 62, 63, and 64? (see Fig. 2B), Gerennavár Limestone Formation, Griesbachian, Lower Triassic.

Family Pachydomellidae Berdan and Sohn, 1961

Genus *Microcheilinella* Geis, 1933

Type species: *Microcheilus distortus* Geis, 1932; Upper Mississippian of Indiana, USA.

Microcheilinella egerensis Forel sp. nov.

Figs. 15Q–X, 16.

Etymology: In reference to the city of Eger, Hungary.

Type material: Holotype: one complete carapace, Fig. 15Q, UPMC P6M2879, sample 08BAN61. Paratype: one complete carapace, Fig. 15S, UPMC P6M2881, sample 08BAN61.

Type locality: Bálvány North section, Bükk Mountains, Hungary.

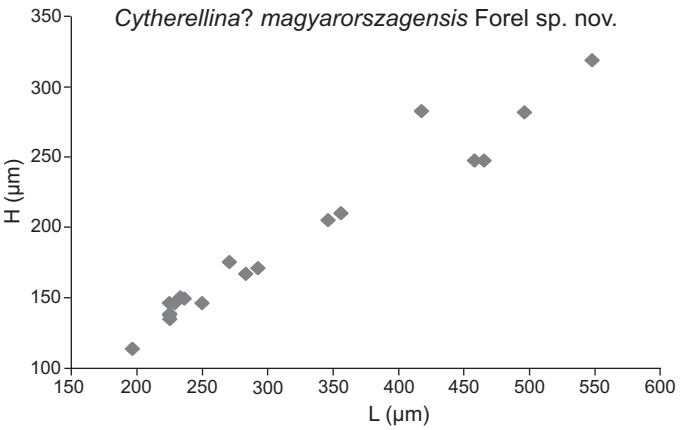

Fig. 14. Height/length diagram of *Cytherellina*? *magyarorszagensis* Forel sp. nov.

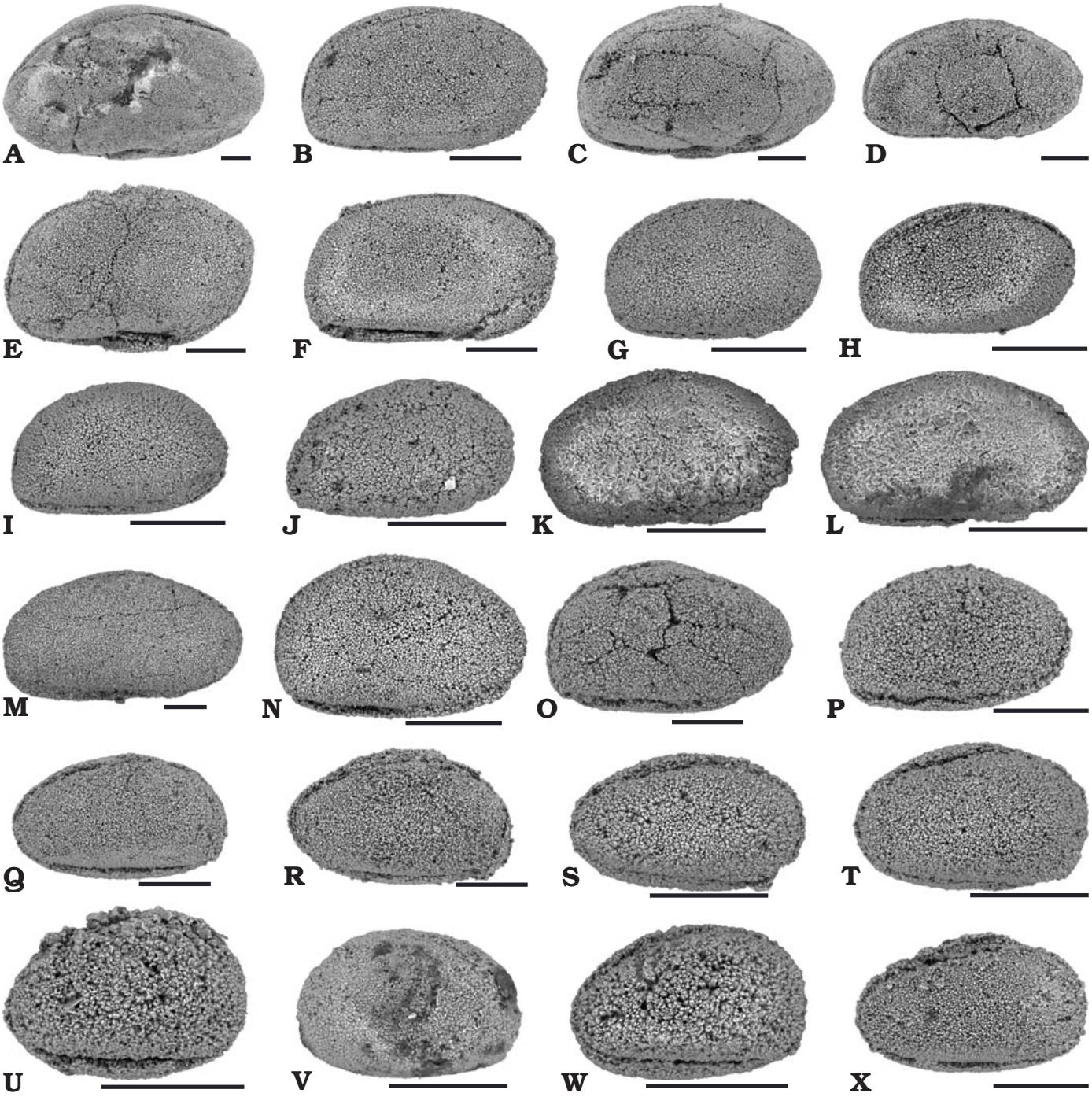

Fig. 15. Ostracods from Bálvány North section, Bükk Mountains, Hungary. Right lateral views of complete carapaces. **A**. *Bairdiacypris* cf. *fornicata* Shi, 1982, UPMC P6M2863, sample 08BAN47, Upper Permian. **B**–**J**. *Cytherellina*? *magyarorszagensis* Forel sp. nov., Griesbachian, Lower Triassic. **B**. Holotype, UPMC P6M2864, sample 08BAN63. **C**. Paratype, UPMC P6M2865, sample 08BAN61. **D**. UPMC P6M2866, sample 08BAN61. **E**. UPMC P6M2867, sample 08BAN63. **F**. UPMC P6M2868, sample 08BAN63. **G**. UPMC P6M2869, sample 08BAN62. **H**. UPMC P6M2870, sample 08BAN61. **I**. UPMC P6M2871, sample 08BAN62. **J**. UPMC P6M2872, sample 08BAN62. **K**, **L**. *Cytherellina*? sp. E, Changhsingian, Upper Permian. **K**. UPMC P6M2873, sample 08BAN47. **L**. UPMC P6M2874, sample 08BAN47. **M**–**P**. *Hungarella gerennavarensis* Crasquin sp. nov., Griesbachian, Lower Triassic. **M**. Holotype, UPMC P6M2875, sample 08BAN62. **N**. Paratype, UPMC P6M2876, sample 08BAN67. **O**. UPMC P6M2877, sample 08BAN63. **P**. UPMC P6M2878, sample 08BAN63. **Q**–**X**. *Microcheilinella egerensis* Forel sp. nov., Griesbachian, Lower Triassic. **Q**. Holotype, UPMC P6M2879, sample 08BAN61. **R**. UPMC P6M2880, sample 08BAN63. **S**. Paratype, UPMC P6M2881, sample 08BAN61. **T**. UPMC P6M2882, sample 08BAN62. **U**. UPMC P6M2883, sample 08BAN61. **V**. UPMC P6M2884, sample 08BAN61. **W**. UPMC P6M2885, sample 08BAN63. **X**. UPMC P6M2886, sample 08BAN61. Scale bars 100 μm.

Type horizon: Level 7, Gerennavár Limestone Formation, Griesbachian, Lower Triassic.

Material.—35 complete and 5 broken carapaces, samples 08BAN61, 62, 63, and 67 (see Fig. 2B), levels 7, 8, Gerenna-

http://dx.doi.org/10.4202/app.2011.0126

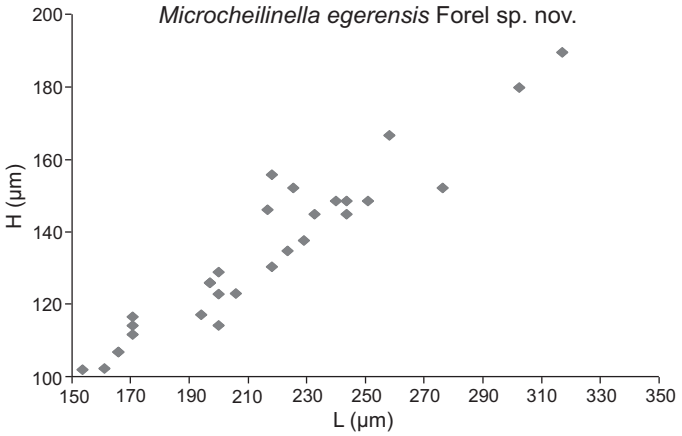

Fig. 16. Height/length diagram of *Microcheilinella egerensis* Forel sp. nov.

vár Limestone Formation, Bálvány North section, Hungary, Griesbachian, Lower Triassic.

Diagnosis.—A species of *Microcheilinella* with a quadrant-shaped AB and a PB with quite large radius of curvature; VB and DB of both valves nearly straight.

Dimensions.—L 155–395 µm; H 100–250 µm (see Fig. 16).

Description.—Carapace moderately elongated (H/L 0.60); LV: DB gently convex to straight; AB with quite large radius of curvature (particularly in larval stages) and ventral part quite vertical; VB slightly convex to straight; PB regularly rounded with maximum of curvature located close to mid-H; RV: DB straight and inclined backwards; anterior part of the carapace in shape of a quadrant, quite vertical in ventral part; VB straight; PB equivalent to PB of LV;

LV overlaps RV all around the carapace; relative weak overlap with a maximum located at posterior part of DB; hinge line invaginated; larval stages show a larger AB than adults. Internal features unknown.

Discussion.—*Microcheilinella egerensis* sp. nov. is quite close to two species described from the Upper Permian of the Meishan section (Crasquin et al. 2010a), *Microcheilinella shicheni* Crasquin, 2010 and *Microcheilinella rectodorsata* Forel, 2010, both from the Changhsingian. *M. shicheni* has a PB with a smaller radius of curvature, a convex DB in both valves and more-or-less parallel and horizontal DB and VB. *M. rectodorsata* has quite the same shape at the AB but PB shows a smaller radius of curvature and the carapace is more elongated. *M. hungarica* Kozur, 1985 from the Lower Wuchiapingian of Bükk Mountains (Kozur 1985b) is longer and has a more slender PB particularly in RV.

Very few species of *Microcheilinella* are recorded from the Triassic: *M*. sp. from the Spathian of Pakistan (Sohn 1970), *M.* cf. *venusta* Chen, 1958 and *M.*? sp. 1 sensu Crasquin-Soleau et al. (2006) from the Spathian of Guangxi. They belong to the survivors of the PTB mass extinction.

Stratigraphic and geographic range.—Bálvány North section, levels 7, 8, samples 08BAN61, 62, 63, and 67 (see Fig. 2B), Gerennavár Limestone Formation, Griesbachian, Lower Triassic.

Family Bythocytheridae Sars, 1926

Genus *Callicythere* Wei, 1981

Type species: *Callicythere emeiensis* Wei, 1981; Lower Triassic, Sichuan Province, China

Callicythere? *balvanyseptentrioensis* Forel sp. nov.

Figs. 17, 18A–H.

Etymology: Latinization of Bálvány North section.

Type material: Holotype: one complete carapace, Fig. 18A, UPMC P6M2900, sample 08BAN62. Paratype: one complete carapace, Fig. 18B, UPMC P6M2901, sample 08BAN61.

Type locality: Bálvány North section, Bükk Mountains, Hungary.

Type horizon: Level 8, Gerennavár Limestone Formation, Griesbachian, Lower Triassic.

Material.—44 complete and 11 broken carapaces, samples 08BAN47, 50, 59, 61, 62, 63, 64, 67, and 69 (see Fig. 2B), levels 1, 5, 7, 8, Nagyvisnyó and Gerennavár Limestone Formations, Bálvány North section, Hungary, Changhsingian to Griesbachian, Upper Permian–Lower Triassic.

Diagnosis.—A species attributed with doubt to *Callicythere* with a small radius of curvature at the PB, without S_2 and dorsolateral furrow.

Dimensions.—L 180–345 µm; H 110–210 µm (see Fig. 17).

Description.—Carapace quite equivalve with surface smooth without S_2 nor narrow furrow; sexual dimorphism is well-expressed. Heteromorphs: DB convex; AB laterally compressed with large radius of curvature and maximum of convexity located at or below mid-H; VB straight and overreached by posteroventral wing-like inflation; PB laterally flattened with quite large radius of curvature and maximum of convexity located at or below mid-H; Hmax located at anterior part of DB. Tecnomorphs: DB straight to gently convex; AB laterally compressed with large radius of curvature and maximum of convexity located at or below mid-H; VB as in females; PB as in females but with smaller radius of curvature; Hmax located at anterior part of DB; carapace in dorsal view thinner than females. Internal features unknown.

Discussion.—Wei (1981) included the genus *Callicythere* in

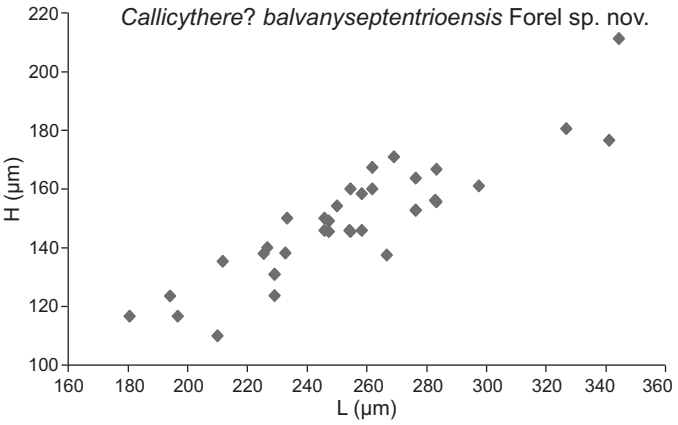

Fig. 17. Height/length diagram of *Callicythere*? *balvanyseptentrioensis* Forel sp. nov.

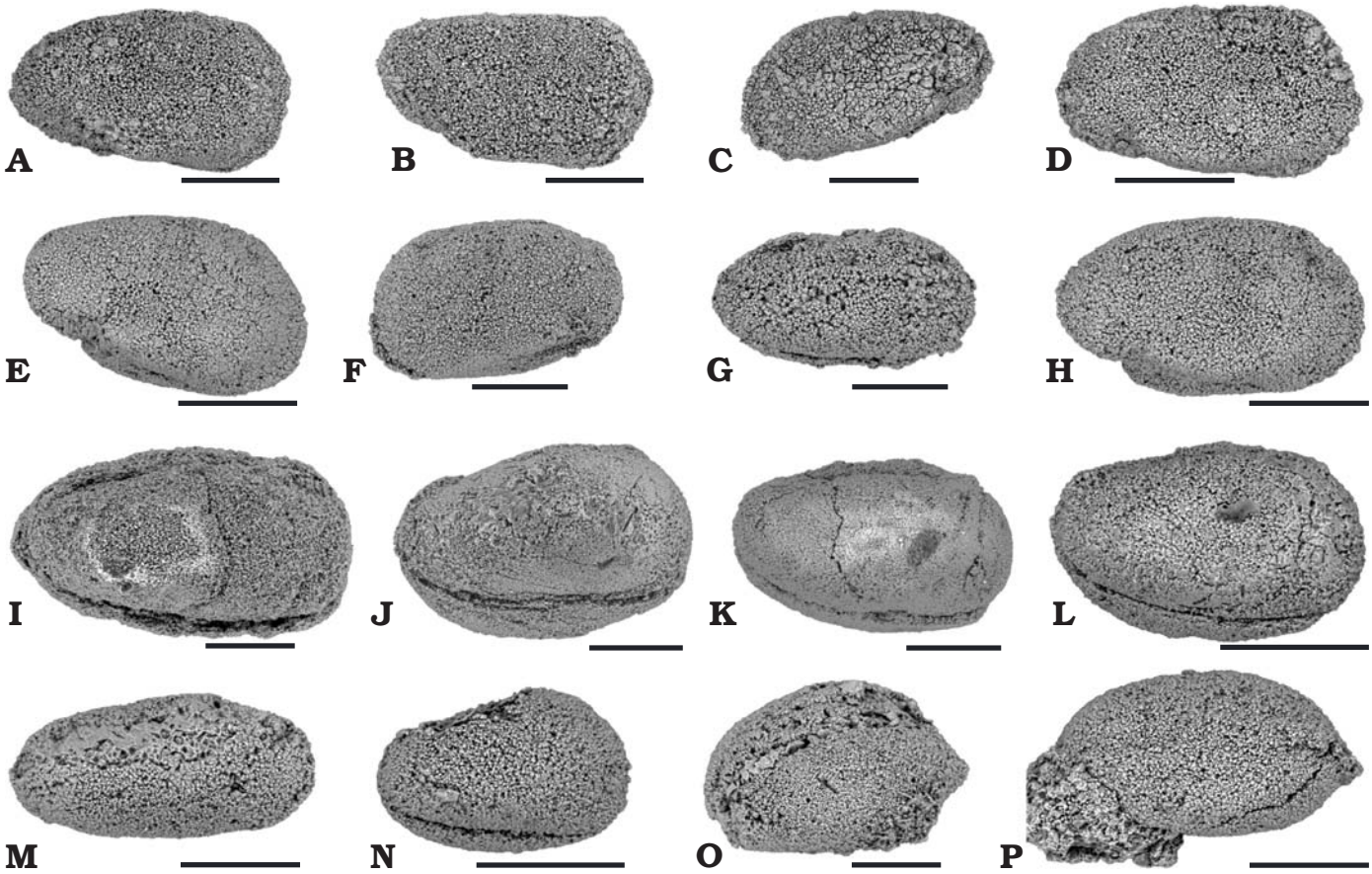

Fig. 18. Ostracods from Bálvány North section, Bükk Mountains, Hungary. Right (A, B, D, E, G–P) and left (C, F) lateral views of complete carapaces. **A**–**H**. *Callicythere*? *balvanyseptentrioensis* Forel sp. nov., Griesbachian, Lower Triassic. **A**. Holotype, UPMC P6M2900, sample 08BAN62. **B**. Paratype, UPMC P6M2901, sample 08BAN61. **C**. UPMC P6M2902, sample 08BAN62. **D**. UPMC P6M2903, sample 08BAN62. **E**. UPMC P6M2904, sample 08BAN62. **F**. UPMC P6M2905, sample 08BAN63. **G**. UPMC P6M2906, sample 08BAN64. **H**. UPMC P6M2907, sample 08BAN62. **I**–**L**. *Eumiraculum desmaresae* Forel sp. nov., Changhsingian, Upper Permian. **I**. UPMC P6M2908, sample 08BAN47. **J**. Holotype, UPMC P6M2909, sample 08BAN47. **K**. Paratype, UPMC P6M2910, sample 08BAN47. **L**. UPMC P6M2911, sample 08BAN47. **M**. *Sulcella*? sp., UPMC P6M2916, sample 08BAN67, Griesbachian, Lower Triassic. **N**. *Eumiraculum* cf. *Eumiraculum desmaresae* Forel sp. nov., UPMC P6M2912, sample 08BAN67, Griesbachian, Lower Triassic. **O**, **P**. *Cetollina*? sp. A. **O**. UPMC P6M2913, sample 08BAN59, Changhsingian, Upper Permian. **P**. UPMC P6M2914, sample 08BAN66, Griesbachian, Lower Triassic. Scale bars 100 μm.

the Family Cytherissinellidae Kashevarova, 1958. It seems that this attribution is due to the similarity between *Callicythere* and *Lutkevichinella* Schneider, 1956 (for discussion see Wei 1981: 506). The description of the Family Cytherissinellidae is: "elongate suboblong, dorsal margin straight, anterior and posterior ends rounded, with faint to distinct narrow sulcus extending straight downward from mid-dorsal region; surface reticulated and may bear inconspicuous longitudinal ribs." (Moore 1961: Q290–Q292). In the description of *Callicythere,* Wei (1981) pointed out "… shallow V-shaped depression, on mid-dorsal region". Because of this "V-shaped depression", close to a true S_2, and the presence of latero-ventral structures we attribute this genus to the Bythocytheridae Sars, 1926. The doubt about the generic attribution of our new species is due to the absence (or non-preservation?) of a dorso-median depression or sulcus.

Callicythere? *balvanyseptentrioensis* sp. nov. is close to *Callicythere postiangusta* Wei, 1981 from the Lower Triassic of Emei (Sichuan, South China; Wei 1981). The latter species has a PB with a larger radius of curvature and less distinct ACA.

Stratigraphic and geographic range.—Bálvány North section, levels 1, 5, 7, 8, samples 08BAN47, 50, 59, 61, 62, 63, 64, 67, and 69 (see Fig. 2B), Nagyvisnyó and Gerennavár Limestone Formations, Changhsingian to Griesbachian, Upper Permian to Lower Triassic.

Order and suborder indet.

Genus *Eumiraculum* Chen, 1987

Type species: *Eumiraculum changxingensis* Chen, 1987; Uppermost Permian, Meishan section, Zhejiang Province, China.

Eumiraculum desmaresae Forel sp. nov.

Figs. 18I–L, 19.

Etymology: Dedicated to Dr. Delphine Desmares (UPMC, Paris, France).

http://dx.doi.org/10.4202/app.2011.0126

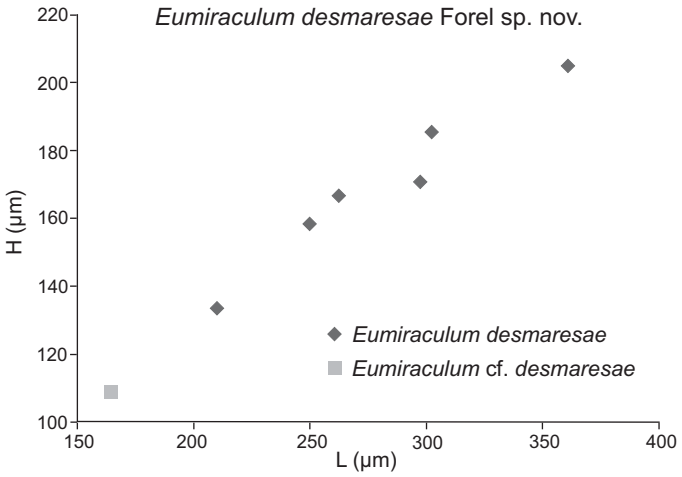

Fig. 19. Height/length diagram of *Eumiraculum desmaresae* Forel sp. nov.

Type material: Holotype: one complete carapace, Fig. 18J, UPMC P6M2909, sample 08BAN47. Paratype: one complete carapace, Fig. 18K, UPMC P6M2910, sample 08BAN47.

Type locality: Bálvány North section, Bükk Mountains, Hungary.

Type horizon: Level 1, Nagyvisnyó Limestone Formation, Changhsingian, Upper Permian.

Material.—6 complete and 1 broken carapaces, sample 08BAN47 (see Fig. 2B), level 1, Nagyvisnyó Limestone Formation, Bálvány North section, Hungary, Changhsingian, Upper Permian.

Diagnosis.—A species of *Eumiraculum* with a small PB, strong overlap of the LV on the RV and a ornamentation very subtle.

Dimensions.—L 210–360 µm; H 135–205 µm (see Fig. 19).

Description.—Carapace massive, strongly inequivalve, ornamentation very subtle on lateral surface of valves; maximum of overlap (LV on RV) at anterior part of DB and VB. LV: DB convex, ACA distinct (about 90°) identical to ACA of RV; PCA not marked; AB regularly rounded, in this part RV overlaps LV; VB convex; PB with small radius of curvature. Internal features unknown. RV: DB concave to straight; ACA(?) well expressed (about 90°) and underlain by a small "spine"; AB with large radius of curvature, maximum of convexity located at mid-H, contact with VB angular (a little more than 90°); VB slightly convex; PB with small radius of curvature and maximum of convexity located above mid-H; link with DB (PCA?) less pronounced than anterior one, small "spine" not clearly visible; RV overlapped by LV all around the carapace except at AB where the overlap is reversed.

Discussion.—*Eumiraculum desmaresae* sp. nov. looks like *Eumiraculum changxingensis* Chen, 1987 from the Upper Changhsingian of Meishan section (Shi and Chen 1987; Crasquin et al. 2010a). At *E. desmaresae* sp. nov. the PB has a smaller radius of curvature, the overlap of the LV on the RV is less significant and the ornamentation is poorly expressed.

Stratigraphic and geographic range.—Bálvány North section, level 1, sample 08BAN47 (see Fig. 2B), Nagyvisnyó Limestone Formation, Changhsingian, Upper Permian.

Remarks on biostratigraphic value of ostracods in this section

Kozur (1985a, b) proposed a zonation based on ostracods for the Upper Palaeozoic of Bükk Mountains. However, in these papers, there is no section with ostracod distribution available. He defined seven ostracod assemblage zones from the Moscovian (middle Upper Carboniferous) to Lower Triassic. Kozur (1985a) defined an "*Indivisia buekkensis* Assemblage Zone" as index of Upper Permian and a "*Hollinella tingi* Assemblage Zone" as index of index of lowermost Triassic. This last assemblage is associated with *Isarcicella isarcica* (Huckriede, 1958), conodont index of lowermost Triassic. The species occurring in the two last assemblage zones, VI "*Indivisia buekkensis* Assemblage Zone" and VII "*Hollinella tingi* Assemblage Zone", which correspond to our data (Table 1). The zones are defined from borehole sediments from Bükk Mountains (see Kozur 1985a). The two species *Indivisia buekkensis* and "*Hollinella tingi*" (*Hollinella tingi* [Patte, 1935] is an Lower Permian species from South China; see the discussion about this last species above and in Crasquin-Soleau et al. 2004a) are not recognized in Bálvány section. *Indivisia symmetrica* Kozur, 1985, which is present in Kozur's (1985a) "*Indivisia buekkensis* Assemblage Zone" was recognized in the upper part of Meishan GSSP section (Crasquin et al. 2010a). This species could be a good marker for the uppermost Changhsingian. *Callicythere mazurensis* (Styk, 1972) which is present in "*Hollinella tingi* Assemblage Zone" was recognized in the Upper Changhsingian of Bulla section (North Italy, Crasquin et al. 2008). Some species could be considered as Upper Changhsingian index in

Table 1. Upper Permian (VI) and Lower Triassic (VII) ostracod assemblage zones of Kozur (1985a). Asterisked is a species which actually is present before its "assemblage zone".

Ostracod assemblage zones	Ostracod species in assemblage zones (Kozur 1985a: table 2)	Ages
VII: "*Hollinella tingi* Assemblage Zone"	*Callicythere mazurensis* (Styk, 1972)	lowermost Triassic
	Cavellina sp.	
	Hollinella tingi (Patte, 1935)	
	Liuzhinia sp.	
VI: "*Indivisia buekkensis* Assemblage Zone"	*Indivisia buekkensis* Kozur, 1985	uppermost Changhsingian
	Indivisia symmetrica Kozur, 1985	
	**Judahella bogschi bogschi* Kozur, 1985	
	Praepilatina sp.	

Fig. 20. **A**. Lithostratigraphy and ostracod fauna evolution at Bálvány North section. For legend of lithology see Fig. 2. **B**. Variation of the number of species (continuous line) and specimens (dashed line). **C**. Percentage of bioclasts in thin sections of samples from the Bálvány North section, from Haas et al. (2006). →

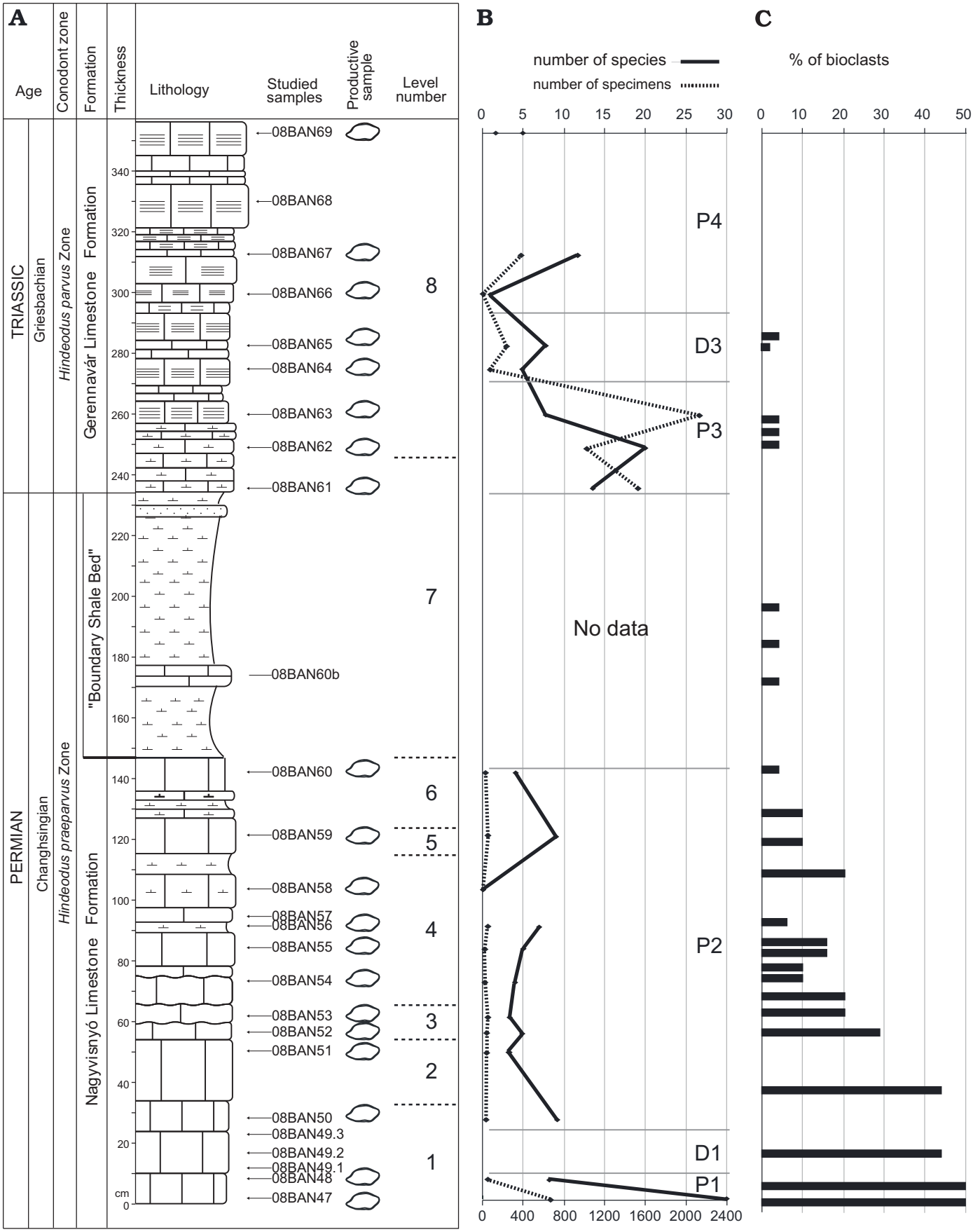

http://dx.doi.org/10.4202/app.2011.0126

Bálvány section: *Eumiraculum desmaresae* Forel sp. nov., *Acratia nagyvisnyoensis* Forel sp. nov., *Reviya praecurukensis* Forel sp. nov., *Hollinella fengqinglaii* Crasquin sp. nov. For the Lower Griesbachian, the following species could be good biochronometers, at least locally: *Cytherellina*? *magyarorszagensis* Forel sp. nov., *Langdaia bullabalvanyensis* Crasquin sp. nov.

Ostracod biodiversity and ecological variation

Ostracods are found from the top of the Nagyvisnyó Formation (lowest occurrence in sample 08BAN47) to the base of the Gerennavár Formation (highest occurrence in sample 08BAN69). Consequently, ostracods are present from the upper *Hindeodus praeparvus* Conodont Zone to the lower *Hindeodus parvus* Zone (Figs. 2A, 20).

Nineteen of the twenty-five samples collected from this interval yielded ostracods (Fig. 2A). The species distribution is given in Fig. 2B; abundance and species richness are presented in Fig. 20A. In productive samples, specific richness varies from 1 (08BAN66) to 28 (08BAN47) species and abundance from 4 (08BAN66) to 2135 (08BAN63) specimens. In most assemblages the variation of species richness correlates with the abundance. Only the samples 08BAN62 and 08BAN63 record a strong disparity between the abundance (increase from 1017 to 2135) and the number of species (decrease from 20 to 8). Assemblages of the Gerennavár Formation (08BAN61 to 08BAN69) show a higher abundance than the samples of the Nagyvisnyó Formation (08BAN47 to 08BAN60). Based on the iridium content, a change of sedimentation rate seems to occur at the transition between the uppermost beds of the Nagyvisnyó Formation and the lower part of the Boundary Shale Beds (Haas et al. 2007). Therefore we consider that changes in the sedimentation rate do not influence the diversity of our assemblages. However, we did not sample the BSB because of the siliciclastic lithology. We observed carefully the rocks with lens on field and we haven't seen any ostracods. The extinction rates from the Permian to the Triassic at the Bálvány North section show particularities. The number of superfamilies/ families does not change from the Permian to the Triassic, although a decrease is recorded for the number of genera (from 17 to 14 genera) and species (from 54 to 36 species). The specific extinction rate is 74% (40 species extinct at PTB). Thus, at the Bálvány North section, the loss of ostracod diversity is confined to the genus and species levels. The species extinction rate at Bálvány North is significantly lower than the 99% recorded at Meishan section, GSSP of the PTB (Zhejiang Province, South China; Crasquin et al. 2010a; Forel et al. 2011; Crasquin and Forel in press). Fourteen species cross the PTB. On 36 Griesbachian species, 22 are new and document a specific turnover rate of about 61% in Bálvány North. This specific turnover is 67% in Meishan (but only 3 species are recognized) and 90% in Bulla (Italian Dolomites) (Crasquin and Forel in press). Two successive patterns can be distinguished here among the surviving species (Fig. 2B): the first one is documented by species which cross the PTB but disappear a few centimetres above the PTB; the second one is recorded by 7 (?9) species with a longer range within the Lower Triassic. It reflects 2 successive phases of survival for the ostracods, which are associated with the microbialites at the Bálvány North section:

- 24 ostracod species are recorded in the first 30 centimetres of the Triassic Formation, including 13 species, which are not present in Permian beds. In this portion of the Gerennavár Formation, the faunal renewal is close to 54%.
- 26 species are found in the upper part of the microbialites, including 17, which are not present in the Permian beds. This indicates a relative faunal renewal of about 47% for the upper part of the section.

The curve illustrating the variations of ostracod diversity (both species richness and abundance) can be divided into successive peaks (P) and drops (D) (Fig. 20A):

- The maximum of species diversity is recorded at the base of the section by the assemblages 08BAN47 and 08BAN48 (P1: 28 species in 08BAN47).
- Ostracods are absent from 08BAN49.1, 49.2, 49.3 (D1).
- Assemblages from 08BAN50 to 08BAN60 show a slight rediversification, reaching medium values of species richness (P2).
- Above the BSB, assemblages from the base of the Gerennavár Formation (08BAN61 to 08BAN63) are characterised by an increase of the species richness and abundance (P3). The maximal abundance is reached in 08BAN63 (2135 specimens).
- The assemblages 08BAN64 and 08BAN65 record a reduction of diversity (D3).
- A slight rediversification is recorded at the top of the sampled part of the Gerennavár Formation (P4: 08BAN66 to 08BAN69).

The samples 08BAN49.1, 49.2, 49.3, 57, 58, 68 yielded no ostracods. This absence of ostracods can be explained by (i) their initial absence at the time of deposition, implying a harsh environment, (ii) the displacement of the carapaces by current activity, (iii) the non-preservation or dissolution of carapaces. However, because most of the specimens recovered are closed carapaces, we assume the transportation to be limited (Oertli 1971). Note that instars (larval stages) are present for many species which also indicates, more strongly, that these taxa are in-situ (e.g., Boomer et al. 2003). Moreover, according to recent comparative analysis of ostracod extraction protocols, the method used in our study has limited dissolution effects on microfossils (Rodrigues et al. 2012). To conclude, the non-productive samples come from levels of homogeneous lithologies, where surrounding samples are productive. The absence of ostracods seems not to be linked to facies particularities. Therefore, we consider the assemblages observed as autochthonous and relatively representative of the biocoenosis.

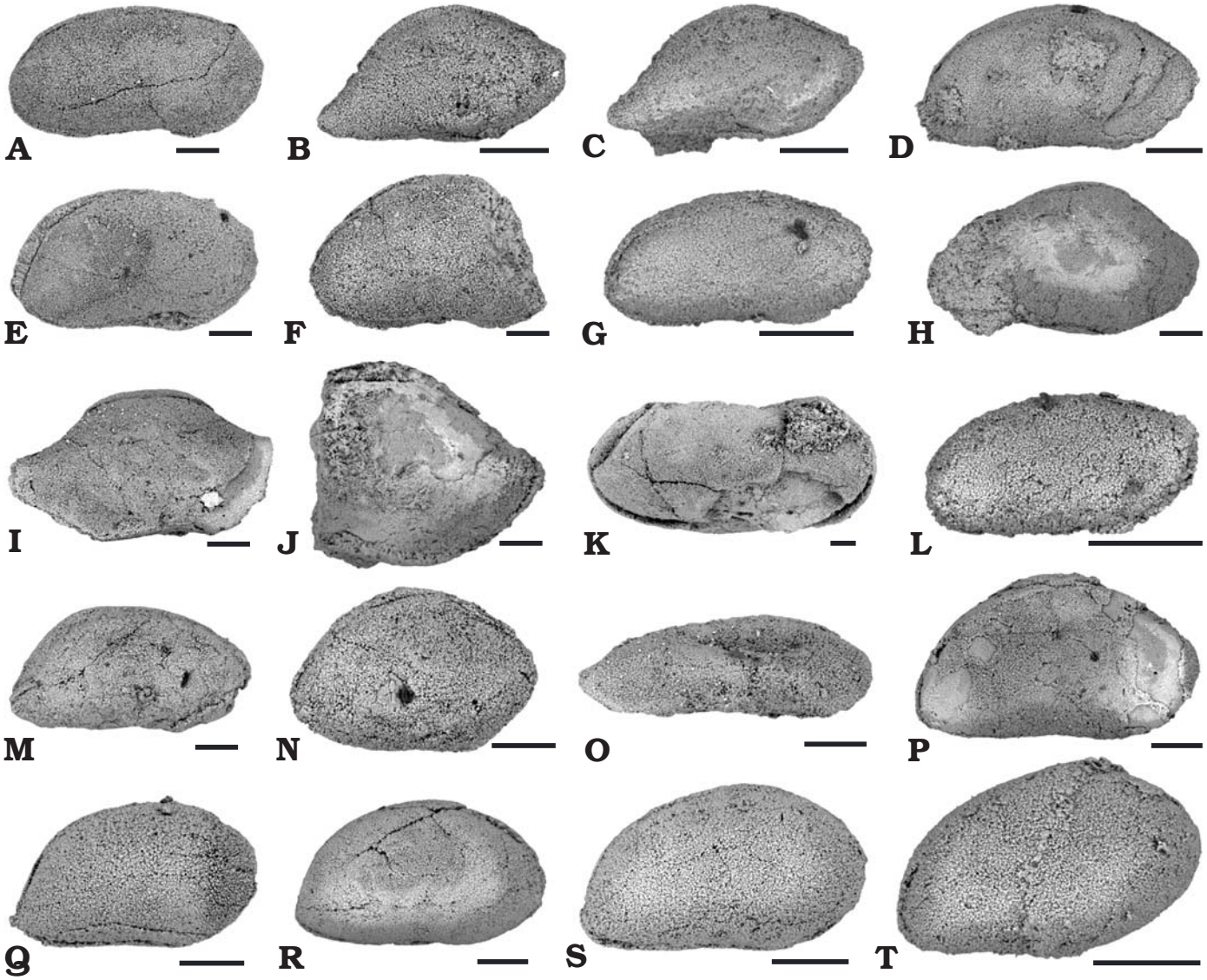

Fig. 21. Ostracods from Bálvány North section, Bükk Mountains, Hungary. Right lateral views of complete (A–I, L–T) and broken (J, K) carapaces. **A**. *Bairdia* cf. *broutini* Crasquin, 2010a. UPMC P6M2784, sample 08BAN62, Griesbachian, Lower Triassic. **B–C**. *Bairdia* cf. *urodeloformis* Chen, 1987, Changhsingian, Upper Permian. **B**. UPMC P6M2768, sample 08BAN47. **C**. UPMC P6M2769, sample 08BAN47. **D**. *Bairdia* sp. A sensu Crasquin et al. (2010), UPMC P6M2787, sample 08BAN47, Changhsingian, Upper Permian. **E**. *Bairdia* sp. F, UPMC P6M2788, sample 08BAN62, Griesbachian, Lower Triassic. **F**. *Bairdia* sp. G, UPMC P6M2838, sample 08BAN54, Changhsingian, Upper Permian. **G**. *Bairdia* sp. H, UPMC P6M2789, sample 08BAN47, Changhsingian, Upper Permian. **H**. *Bairdia* sp. I, UPMC P6M2790, sample 08BAN50, Changhsingian, Upper Permian. **I**. *Bairdia* sp. J, UPMC P6M2791, sample 08BAN50, Changhsingian, Upper Permian. **J**. *Bairdia* sp. K, UPMC P6M2792, sample 08BAN59, Changhsingian, Upper Permian. **K**. *Bairdia* sp. L, UPMC P6M2793, sample 08BAN54, Changhsingian, Upper Permian. **L**. *Bairdia* sp. M, UPMC P6M2794, sample 08BAN47, Changhsingian, Upper Permian. **M**. *Bairdia*? sp. N, UPMC P6M2795, sample 08BAN52, Changhsingian, Upper Permian. **N**. *Bairdia* sp. O, UPMC P6M2796, sample 08BAN47, Changhsingian, Upper Permian. **O**. *Bairdia* sp. P, UPMC P6M2797, sample 08BAN48, Changhsingian, Upper Permian. **P**. *Bairdia* sp. Q, UPMC P6M2798, sample 08BAN59, Changhsingian, Upper Permian. **Q**. *Bairdia* sp. R, UPMC P6M2799, sample 08BAN60, Changhsingian, Upper Permian. **R**. *Bairdia* sp. S, UPMC P6M2800, sample 08BAN62, Griesbachian, Lower Triassic. **S**. *Bairdia*? sp. T, UPMC P6M2801, sample 08BAN61, Griesbachian, Lower Triassic. **T**. *Bairdia* sp. U, UPMC P6M2802, sample 08BAN65, Griesbachian, Lower Triassic. Scale bars 100 μm.

A study of the Permian–Triassic interval at the Bálvány North section (Haas et al. 2006) shows a decreasing trend of abundances throughout the sampled part of the Nagyvisnyó Formation on the basis of bioclasts in thin sections (Fig. 20B). This trend and the concurrent disappearance of taxa was considered by Haas et al. (2006) to be directly related to the end-Permian events and not to local facies changes. This hypothesis can be tested by the present ostracod diversity record.

The highest species richness of ostracod assemblages is recorded at the base of the section (sample 08BAN47, P1) and is correlated with the maximum of bioclast abundance. The ostracod data following upsection show lower species richness and a very low abundance, in accordance with the

http://dx.doi.org/10.4202/app.2011.0126

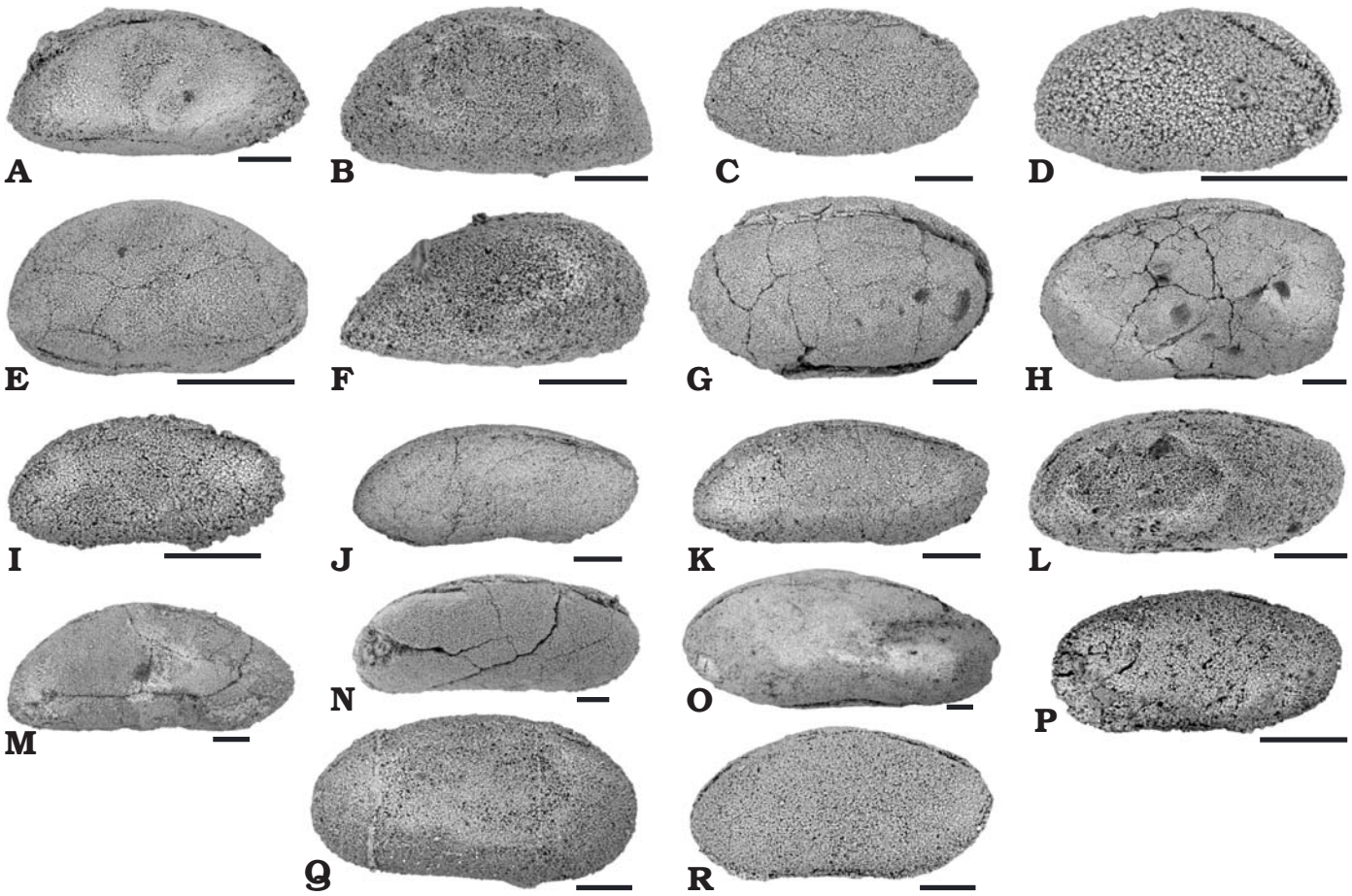

Fig. 22. Ostracods from Bálvány North section, Bükk Mountains, Hungary. Right lateral view of complete carapaces, except B. **A**. *Acratia* cf. sp. C. UPMC P6M2823, sample 08BAN53. **B**. *Acratia* sp. D. UPMC P6M2824, sample 08BAN47. **C**. *Acratia*? sp. E. UPMC P6M2825, sample 08BAN55. **D**. *Acratia* sp. F. UPMC P6M2826, sample 08BAN67. **E**. *Kempfina*? sp. A. UPMC P6M2827, sample 08BAN47. **F**. *Baschkirina* cf. *huzhouensis* Forel, 2010. UPMC P6M2828, sample 08BAN47. **G**, **H**. ?*Bairdiacypris caeca* Shi, 1987. **G**. UPMC P6M2829, sample 08BAN59. **H**. UPMC P6M2830, sample 08BAN59. **I–L**. *Fabalicypris parva* Wang, 1978. **I**. UPMC P6M2835, sample 08BAN47. **J**. UPMC P6M2832, sample 08BAN47. **K**. UPMC P6M2833, sample 08BAN47. **L**. UPMC P6M2834, sample 08BAN47. **M**. *Fabalicypris arcuata* Wang, 1978. UPMC P6M2831, sample 08BAN51. **N**. *Fabalicypris* cf. *parva* Wang, 1978. UPMC P6M2836, sample 08BAN61. **O**. *Fabalicypris reniformis* (Chen, 1958) sensu Wang, 1978. UPMC P6M2837, sample 08BAN48. **P**, **R**. *Fabalicypris* cf. *elliptica rotunda* Kozur, 1985. **P**. UPMC P6M2839, sample 08BAN47. **R**. UPMC P6M2840, sample 08BAN62. **Q**. *Fabalicypris*? sp. UPMC P6M2841, sample 08BAN53. Scale bars 100 μm.

bioclast abundance pattern. However, this trend of diversity reduction is gradual for bioclast abundance whereas it is sharp for the ostracod diversity and followed upsection by relatively stable values. We therefore conclude that the bioclast abundance pattern does not reflect the real dynamics of extinction of different organisms.

Another significant discrepancy is recorded at the base of the Gerennavár Formation where bioclasts are rare but ostracod assemblages more abundant (highest abundance in P3, sample 08BAN63) and diversified than those of the Nagyvisnyó Formation. Haas et al. (2006) indicated that packstone laminae with fine fragments of calcareous algae and other bioclasts occur in the stromatolites and interpreted them as storm deposits. In addition to the fact that ostracods are found as closed carapaces, they are found in the entire sampled part of the Gerennavár Formation (except in 08BAN68, Fig. 2A, B). We therefore deduce that their presence does not result from storm current activity but reflects more suitable environmental conditions. An analysis of the composition of assemblages documents their relative homogeneity with respect to superfamilies and families in the entire microbialite succession (Forel et al. 2013). Thus, the abundance pattern at the base of the stromatolites of the Bálvány North section is suggested to be due to special environmental conditions.

The ostracods we describe here through the Permian–Triassic interval in the Bálvány North section show 2 unusual features: (i) high abundance and diversity, in contrast with earlier studies of ostracod faunas at the very base of the Griesbachian which all document impoverished faunas (e.g., South China, Crasquin and Kershaw 2005; Crasquin-Soleau et al. 2006; Crasquin et al. 2010a; Forel and Crasquin 2011b; Tibet: Forel and Crasquin 2011a; Forel et al. 2011; Iran: Mette 2008); (ii) a lower extinction rate than the ostracods at Meishan section (Crasquin et al. 2010a; Forel et al. 2011). Lower

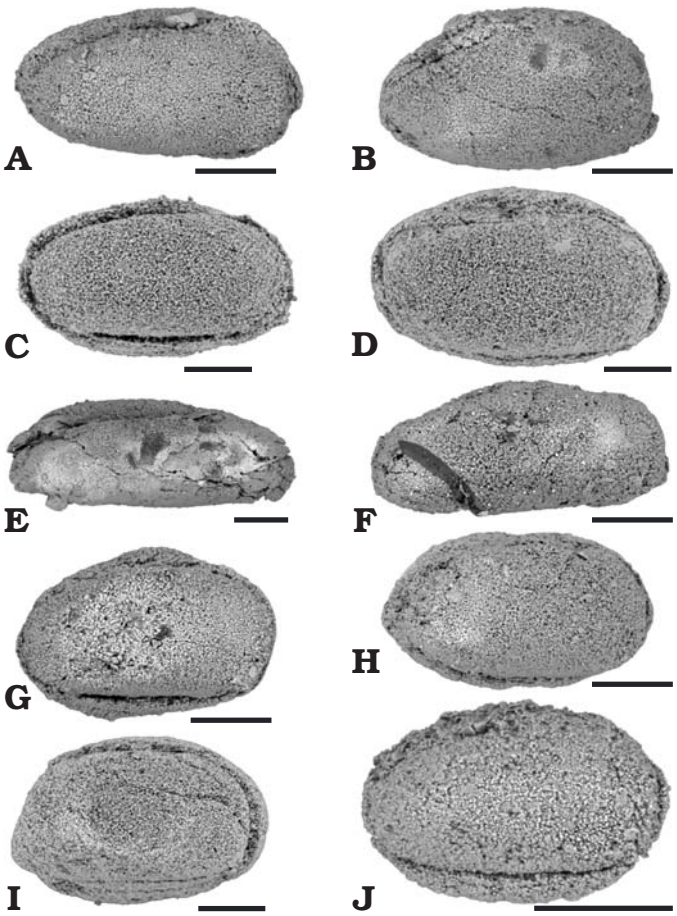

Fig. 23. Ostracods from Bálvány North section, Bükk Mountains, Hungary. Right lateral views of complete carapaces. **A**, **B**. *Microcheilinella* cf. *rectodorsata* Forel, 2010, Changhsingian, Upper Permian. **A**. UPMC P6M2889, sample 08BAN47. **B**. UPMC P6M2890, sample 08BAN47. **C**, **D**. *Microcheilinella* sp. C, Griesbachian, Lower Triassic. **C**. UPMC P6M2891, sample 08BAN61. **D**. UPMC P6M2892, sample 08BAN61. **E**, **F**. *Microcheilinella* sp. D, Changhsingian, Upper Permian. **E**. UPMC P6M2893, sample 08BAN 59. **F**. UPMC P6M2894, sample 08BAN59. **G**, **I**. *Microcheilinella* sp. E, Griesbachian, Lower Triassic. **G**. UPMC P6M2896, sample 08BAN61. **I**. UPMC P6M2897, sample 08BAN61. **H**. *Microcheilinella* sp. F, UPMC P6M2898, sample 08BAN47, Changhsingian, Upper Permian. **J**. *Microcheilinella* sp. G, UPMC P6M2899, sample 08BAN47, Changhsingian, Upper Permian. Scale bars 100 μm.

Triassic beds in Meishan were interpreted as deep external platform deposits (Zhang et al. 2007) of poorly oxygenated to anoxic setting (Wignall and Hallam 1993). This oxygen deficiency in a basinal environment is supported by the absence of ostracods in the Induan of the West Pingdingshan section (Chaohu, Anhui Province; Tong et al. 2005). The two first authors of this paper processed more than one hundred and fifty samples from the Griesbachian–Dienerian part of the Yinkeng Formation and no ostracods were discovered. Lower Triassic beds in Meishan were accumulated at greater water depth than the Lower Triassic beds at the the Bálvány North section (see below for details). These discrepancies between ostracod records are related to more hospitable conditions in Bálvány North provided by the microbial ecosystem from which the microbialites originate. These refuges are documented from several localities and may have prevented the oxygen depletion reaching levels lethal for ostracods (Forel et al. 2013).

Crasquin et al. (2010a) also suggested that the ostracod diversity variations in the Upper Permian of Meishan may be due to the changes in stability/instability of environments as result of sea level changes. Accordingly, increase is linked to stable conditions during high sea-level. Forel and Crasquin (2011b) refined this one-parameter model with data from the Lower Triassic of Meishan. According to Haas et al. (2004), the complete succession at the Bálvány North section was accumulated in an outer ramp setting with a deepening upward trend (Hips and Haas 2009). The important drop in ostracod diversity at the transition from interval P1 to D1 (level 1) could reflect the onset of instability, but the lithofacies do not record such environmental modifications. Stable environmental conditions due to great water depth are recorded at level 4 of the Nagyvisnyó Formation (Hips and Pelikan 2002; Haas et al. 2004, 2006). This environmental stability is indicated by the lack of distinct ostracod diversity changes, which agrees with the suggestion of Crasquin et al. (2010a). The diversity increase at the base of the Gerennavár Formation could be related in first approximation to the stability of the subtidal environment. However, because of the refuge conditions provided by Lower Triassic microbial mats, it seems unlikely to relate ostracod diversity variations within the microbialites to stability conditions. Indeed, the onset of microbial growth marks the transition between: (i) ostracod faunas mainly forced by external parameters (stability/instability related to hydrodynamism and oxygenation) in the Upper Permian Nagyvisnyó Formation; and (ii) faunas whose dynamic is entirely linked to internal parameters associated with the microbial ecosystem functioning (food and oxygen supply by microbes) in the Lower Triassic Gerennavar Formation.

The ostracods of Bükk Mountains (Hungary) present a special behaviour in the general landscape of the PTB interval. Indeed, they have here the lowest specific extinction rate (74%) of all the reference sections studied for ostracod analysis (Crasquin and Forel in press). Furthermore, the fauna exhibits an important endemism. Only 13 species are common with other areas. These palaeobiogeographical particularities of the Hungarian section will be considered in a forthcoming work.

Acknowledgments

We thank the authorities of the Bükk National Park for allowing us to sample and Attila Bartha for leading us in the National Park. We thank Martine Fordant (UPMC) for processing samples and the preparation of ostracods and Alexandre Lethiers (UPMC) for preparing the drawings and plates. We are indebted to Avi Honigstein (Israel Geological Survey, Yerusalem, Israel), Heinz Kozur (Budapest, Hungary), Alan Lord (Senkenberg Museum, Frankfurt, Germany), and Wolfgang Mette (University of Innsbruck, Austria) for their reviewing and their help to

http://dx.doi.org/10.4202/app.2011.0126

improve our manuscript. This work is part of the IGCP 572 "Restoration of Marine Ecosystems following the Permian–Triassic Mass Extinction: lessons for the present". The field work was carried out with the support of 2011 MNHN ATM "Biodiversité actuelle et fossile. Crises, stress, restaurations et panchronisme: le message systématique".

References

Boomer, I., Horne, D.J., and Slipper, I.J. 2003. The use of ostracods in palaeoenvironmental studies, or what can you do with an ostracod shell? *In*: L.E. Park and A.J. Smith (eds.), Bridging the Gap—Trends in the Ostracode Biological and Geological Sciences. *Paleontological Society Paper* 9: 153–179.

Bowman, T.E. and Abele, L.G. 1982. Classification of the Recent Crustacea. *In*: L.G. Abele (ed.), Systematics, the Fossil Record, and Biogeography. *The Biology of Crustacea* 1: 1–27.

Chen, T.C. 1958. Permian ostracods from the Chihsia limestone of Lungtan, Nanking. *Acta Palaeontologica Sinica* 6: 235–257.

Coryell, H.N. 1928. Some new Pennsylvanian Ostracoda. *Journal of Paleontology* 2: 377–381.

Crasquin, S. and Forel, M.B. (in press). Ostracods (Crustacea) through Permian–Triassic events. *Earth-Science Reviews*.

Crasquin, S., Forel, M.-B., Feng, Q., Yuan, A., Baudin, F., and Collin, P.Y. 2010a. Ostracods (Crustacea) through Permian–Triassic boundary in South China: the Meishan stratotype (Zhejiang Province). *Journal of Systematic Palaeontology* 8: 331–370.

Crasquin, S., Perri, M.C., Nicora, A., and De Wever, P. 2008. Ostracods across the Permian–Triassic boundary in Western Tethys: the Bulla parastratotype (Southern Alps, Italy). *Rivista Italiana di Paleontologia e Stratigrafia* 114: 233–262.

Crasquin, S., Shen, S.Z., Li, W.Z., and Cao, C.Q. 2007. Ostracods from the Lopingian and the Permian–Triassic boundary beds at the Gyanyima section in southwestern Tibet, China. *Palaeoworld* 16: 222–232.

Crasquin, S., Sudar, M., Jovanovic, D., and Kolar-Jurkovsek, T. 2010b. Ostracod fauna from Late Permian of Jadar Block (Vardar Zone, NW Serbia). *Geološki anali Balkanskoga poluostrva* 71: 23–35.

Crasquin-Soleau, S. and Kershaw, S. 2005. Ostracod fauna from the Permian–Triassic boundary interval of South China (Huaying Mountains, eastern Sichuan Province): palaeoenvironmental significance. *Palaeogeography, Palaeoclimatology, Palaeoecology* 217: 131–141.

Crasquin-Soleau, S., Galfetti, T., Bucher, H., and Brayard, A. 2006. Early Triassic ostracods from Guangxi Province, South China. *Rivista Italiana di Paleontologia e Stratigrafia* 112: 55–75.

Crasquin-Soleau, S., Marcoux, J., Angiolini, L., and Nicora, A. 2004a. Palaeocopida (Ostracoda) across the Permian–Triassic events: new data from South-Western Taurus (Turkey). *Journal of Micropalaeontology* 23: 67–76.

Crasquin-Soleau, S., Marcoux, J., Angiolini, L., Nicora, A., and Bertho, Y. 2004b. New ostracode fauna from Permian–Triassic boundary in Turkey (Taurus, Antalya Nappes). *Micropaleontology* 50: 281–295.

Crasquin-Soleau, S., Richoz, S., Marcoux, J., Angiolini, L., Nicora, A., and Baud, A. 2002. Les événements de la limite Permien–Trias: derniers survivants et/ou premiers recolonisateurs parmi les ostracodes du Taurus (Sud-Ouest de la Turquie). *Comptes Rendus Geosciences* 334: 489–495.

Crasquin-Soleau, S., Vaslet, D., and Le Nindre, Y.M. 2005. Ostracods from Permian–Triassic boundary in Saudi Arabia (Khuff Formation). *Palaeontology* 48: 853–868.

Croneis, C. and Gale, A.S. 1939. New Ostracodes from the Golchonda Formation. *Journal of Science Laboratory, Denison University* 33: 251–295.

Delo, D.M. 1930. Some Upper Carboniferous Ostracoda from the shale basin of Western Texas. *Journal of Paleontology* 4: 152–178.

Erwin, D.H., Bowring, S.A., and Jin, H.G. 2002. The end-Permian mass extinctions. *In*: C. Koeberl and K.G. MacLeod (ed.), Catastrophic Events and Mass Extinctions: Impacts and Beyond. *Geological Society of America Special Paper* 356: 363–383.

Forel, M.B., Crasquin, S., Kershaw, S., and Collin, P.Y. 2013. In the aftermath of the end-Permian extinction: the microbialite refuge. *Terra Nova* (published online).

Forel, M.B. and Crasquin, S. 2011a. In the aftermath of Permian–Triassic boundary mass-extinction: ostracod new species and genus from South Tibet. *Geodiversitas* 33: 247–263.

Forel, M.B. and Crasquin, S. 2011b. Lower Triassic ostracods (Crustacea) from Meishan section, Permian–Triassic GSSP (Zhejiang Province, South China). *Journal of Systematic Palaeontology* 9: 455–466.

Forel, M.-B., Crasquin, S., Kershaw, S., Feng, Q., and Collin, P.Y. 2009. Ostracods (Crustacea) and water oxygenation in earliest Triassic of South China: implications for oceanic events of the end-Permian mass extinction. *Australian Journal of Earth Sciences* 56: 815–823.

Forel, M.B., Crasquin, S., Brühwiler, T., Goudemand, N., Bucher, H., and Baud, A. 2011. Ostracod recovery after Permian–Triassic boundary mass-extinction in South Tibet. *Palaeogeography, Palaeoclimatology, Palaeoecology* 308: 160–170.

Geis, H.L. 1932. Some Ostracodes from the Salem Limestone, Mississippian of Indiana. *Journal of Paleontology* 6: 149–188.

Gerry, E., Honingstein, A., Derin, B., and Flexer, A. 1987. Late Permian Ostracodes of Israel. Taxonomy, distribution and paleogeographical implications. *Senckbergiana lethaea* 68: 197–223.

Guan, S., Sun, Q., Jiang, Y., Li, L., Zhao, B., Zhang, X., Yang, R., and Feng, B. 1978. Subclass Ostracoda. *Paleontological Atlas of Central and South China*, 115–325. Geological Publishing House, Beijing.

Haas, J., Hips, K., Pelikán, P., Zajzon, N., Götz, A.E., and Tardi-Filácz, E. 2004. Facies analysis of marine Permian/Triassic boundary sections in Hungary. *Acta Geologica Hungarica* 47: 297–340.

Haas, J., Demény, A., Hips, K., and Vennemann, T.W. 2006. Carbon isotope excursions and microfacies changes in marine Permian–Triassic boundary sections in Hungary. *Palaeogeography, Palaeoclimatology, Palaeoecology* 237: 160–181.

Haas, J., Demény, A., Hips, K., Zajzon, N., Weiszburg, T., Sudar, M., and Pálfy, J. 2007. Biotic and environmental changes in the Permian–Triassic boundary interval recorded on a western Tethyan ramp in the Bükk Mountains, Hungary. *Global and Planetary Change* 55: 136–154.

Hao, W. 1992. Early Triassic Ostracods from Guizhou. *Acta Micropalaeontologica Sinica* 9: 37–44.

Hao, W. 1994. The development of the Late Permian–Early Triassic ostracod fauna in Guizhou Province. *Geological Review* 40: 87–93.

Hips, K. and Pelikán, P. 2002. Lower Triassic shallow marine succession in the Bükk Mountains, NE Hungary. *Geologica Carpathica* 53 (6): 1–17.

Hips, K. and Haas, J. 2006. Calcimicrobial stromatolites at the Permian–Triassic boundary in a western Tethyan section, Bükk Mountains, Hungary. *Sedimentary Geology* 185: 239–253.

Hips, K. and Haas, J. 2009. Facies and diagenetic evaluation of the Permian–Triassic boundary interval and the basal Triassic carbonates: shallow and deep ramp sections, Hungary. *Facies* 55: 421–442.

Horne, D.J., Cohen, A., and Martens, K. 2002. Taxonomy, Morphology and Biology of Quaternary and living Ostracoda. *In*: J.A. Holmes and A. Chivas (ed.), The Ostracoda: Applications in Quaternary Research. *Geophysical Monograph* 131: 5–36.

Jones, T. R. and Holl, H. B. 1869 Notes on the Palaeozoic bivalve Entomostraca—9: some Silurian species. *Annals and Magazine of Natural History* 4: 211–229.

Kashevarova, N.P. [Kaševarova, N.P.] 1958. New study of ostracod fauna from Upper Permian (Ufimian to Tatarian) of Timor Peninsula and Volga-Ural platform [in Russian]. *Trudy Vsesoûznogo Neftânogo Naučno-Issledovatel'skogo Instituta (VNIGRI)* 115: 302–339.

Kozur, H. 1985a. Biostratigraphic evaluation of the Upper Paleozoic Conodonts, Ostracods and Holothurian Sclerites of the Bükk Mts. Part II: Upper Paleozoic Ostracods. *Acta Geologica Hungarica* 28: 225–256.

Kozur, H. 1985b. Neue Ostracoden-Arten aus dem Oberen Mittelkarbon (Höheres Moskovian), Mittel- und Oberperm des Bükk- Gebirges (N-Ungarn). *Geologisch Paläontologische Mitteilungen Innsbruck* 2: 1–145.

Kozur, H. and Pjatakova, M. 1976. Die Conodontenart *Anchignathodus*

parvis n. sp. eine wichtige Leitform der basalen Trias. *Proceedings of the Koninklijke Nederlandse Academie van Wetenschappen. Series B: Physical Sciences* 79: 123–128.

Less, G., Gulácsi, Z., Kovács, S., Pelikán, P., Pentelényi, L., and Sásdi, L. 2002. *Geological Map of the Bükk Mts*. 1:50000. Hungarian Geological Institute, Budapest.

Lethiers, F., and Crasquin-Soleau, S. 1988. Comment extraire des microfossiles à tests calcitiques de roches calcaires dures. *Revue de Micropaléontologie* 31: 56–61.

McCoy, F. 1844. *A Synopsis of the Characters of the Carboniferous Limestone Fossils of Ireland*. viii + 207 pp. Dublin University Press, Dublin.

Méhes, G. 1911. Über Trias-Ostrakoden aus dem Bakony. *In*: Resultate der Wissenschaftlichen. Erforschung des Balatonsees, vol. 1 (1). *Palaeontologie der Umgebung des Balatonsees* 3 (6): 1–38.

Mette, W. 2008. Upper Permian and lowermost Triassic stratigraphy, facies and ostracods in NW Iran—implications for the P/T extinction event. *Stratigraphy* 5 (2): 205–219.

Moore, R.C. 1961. *Treatise of Invertebrate Paleontology. Part Q. Arthropoda 3, Crustacea, Ostracoda*. 442 pp. Geological Society of America and University of Kansas Press, Boulder.

Oertli, H.J. 1971. The aspect of Ostracode fauna—a possible new tool in petroleum sedimentology. *In*: H.J. Oertli (ed.), Paléoécologie des Ostracodes. Bulletin du Centre de Recherche, SNPA 5 (Supplement): 137–151.

Patte, E. 1935. Fossiles paléozoïques et mésozoïques du Sud Ouest de la Chine. *Palaeontologica Sinica, Serie B* 15 (2): 1–50.

Posenato, R., Pelikán, P., and Hips, K. 2005. Bivalves and Brachiopods near the Permian–Triassic boundary from the Bükk Mountains (Bálvány North section, Northern Hungary). *Rivista Italiana di Paleontologia e Stratigrafia* 111: 217–234.

Rodrigues, G.B., Bom, M.H., and Fauth, G. 2012. Recovery of ostracods in Cretaceous dolomitic carbonate: The efficiency of acetolysis. *Marine Micropaleontology* 92–93: 81–86.

Sars, G.O. 1926. *An Account of the Crustacea of Norway, Vol. 9. Ostracoda, Parts 13 and 14. Cytheridae (continued)*. 209–240 pp. Bergen Museum, Bergen.

Schneider, G.F 1956. Genus *Pseudoleperditia* Schneider, gen. nov. [in Russian]. *In*: L.D. Kiparisova, B.P. Markovskii, and G.P. Radczenko (ed.), *Materialy po paleontologii; novye semeistva i rody, Vsesoûznogo Naučno-Issledovatelskogo Geologičeskogo Instituta (VSEGEI), Materialy, nov. ser.*, 12, *Paleontologiâ*, p. 87.

Shi, C.G. and Chen, D.Q. 1987. The Changhsingian ostracodes from Meishan Changxing, Zhejiang [in Chinese]. *Stratigraphy and Palaeontology of Systemic Boundaries in China; Permian and Triassic Boundary* 1: 23–80.

Shi, C.G. and Chen, D.Q. 2002. Late Permian ostracodes from Heshan and Yishan of Guangxi. *Bulletin of Nanjing Institute of Geology and Paleontology, Academia Sinica* 15: 47–129.

Sohn, I.G. 1961. *Aechminella*, *Amphissites*, *Kirkbyella* and related genera. *United States Geological Survey Professional Paper* 330-B: 107–160.

Sohn, I.G. 1970. Early Triassic marine ostracodes from the Salt Range and Surghar Range, West Pakistan. *In*: B. Kummel and C. Teichert (ed.), *Stratigraphic Boundary Problems: Permian and Triassic of West Pakistan*, 149–206. Department of Geology, University of Kansas, Special publication, Lawrence.

Sohn, I.G. 1971. New Late Mississippian Ostracode genera and species from Northern Alaska. A review of the Paraparchitacea. *Geological Survey Professional Paper* 711A: 1–24.

Sudar, M., Perri, M.C., and Haas, J. 2008. Conodonts across the Permian–Triassic boundary in the Bükk Mountains (NE Hungary). *Geologica Carpathica* 59 (6): 491–502.

Tong, J., Hansen, H.J., Zhao, L.S,. and Zuo, J.X. 2005. A GSSP candidate of Induan–Olenekian Boundary—stratigraphic sequence of the West Pingdingdhan Section, in Chaohu, Anhui Province. *Journal of Stratigraphy* 29 (2): 205–212.

Wang, S.-Q. 1978. Late Permian and Early Triassic ostracods of Western Guizhou and Northeastern Yunnan. *Acta Palaeontologica Sinica* 17: 277–308.

Wei, M. 1981. Early and Middle Triassic Ostracods from Sichuan. *Acta Palaeontologica Sinica* 20: 501–510.

Wignall, P.B. and Hallam, A. 1993. Griesbachian (Earliest Triassic) palaeoenvironmental changes in the Salt Range, Pakistan and southeast China and their bearing on the Permo-Triassic mass extinction. *Palaeogeography, Palaeoclimatology, Palaeoecology* 102: 215–237.

Yi, W.-J. 2004. Ostracodes from the Upper Permian and Lower Triassic at the Kongtongshan scetion of Datian, Fujian. *Acta Palaeontologica Sinica* 43: 556–570.

Yin, H., Wu, S., Ding, M., Zhang, K., Tong, J., Yang, F., and Lai, X. 1996. The Meishan section, candidate of the Global Stratotype Section and Point of Permian–Triassic boundary. *In*: H.F Yin (ed.), *The Paleozoic–Mesozoic Boundary Candidates of the Global Stratotype Section and Point of the Permian–Triassic Boundary*, 31–48. China University of Geosciences Press, Wuhan.

Yin, H., Zhang, K., Tong, J., Yang, Z., and Wu, S. 2001. The global stratotype section and point of the Permian–Triassic boundary (GSSP). *Episodes* 24: 102–114.

Yuan, A., Crasquin, S., Feng, Q., and Gu, S. 2007. Latest Permian deep-water ostracods from Southwestern Guangxi, South China. *Journal of Micropalaeontology* 26: 169–191.

Yuan, A., Crasquin, S., Feng, Q., and Gu, S. 2009. Ostracods from the uppermost Permian siliceous and muddy rocks from Guizhou, Guangxi and Anhui. *Acta Micropalaeontologica Sinica* 26: 385–403.

Zhang, K.X., Tong, J., Shi, G.R., Lai, X., Yu, J., He, W., Peng, Y., and Jin, Y.G. 2007. Early Triassic conodont—palynological biostratigraphy of the Meishan D Section in Changxing, Zhejiang Province, South China. *Palaeogeography, Palaeoclimatology, Palaeoecology* 252: 4–23.

Zheng, S. 1976. Early Mesozoic ostracodes from some localities in South West China. *Acta Palaeontologica Sinica* 15: 77–93.

http://dx.doi.org/10.4202/app.2011.0126